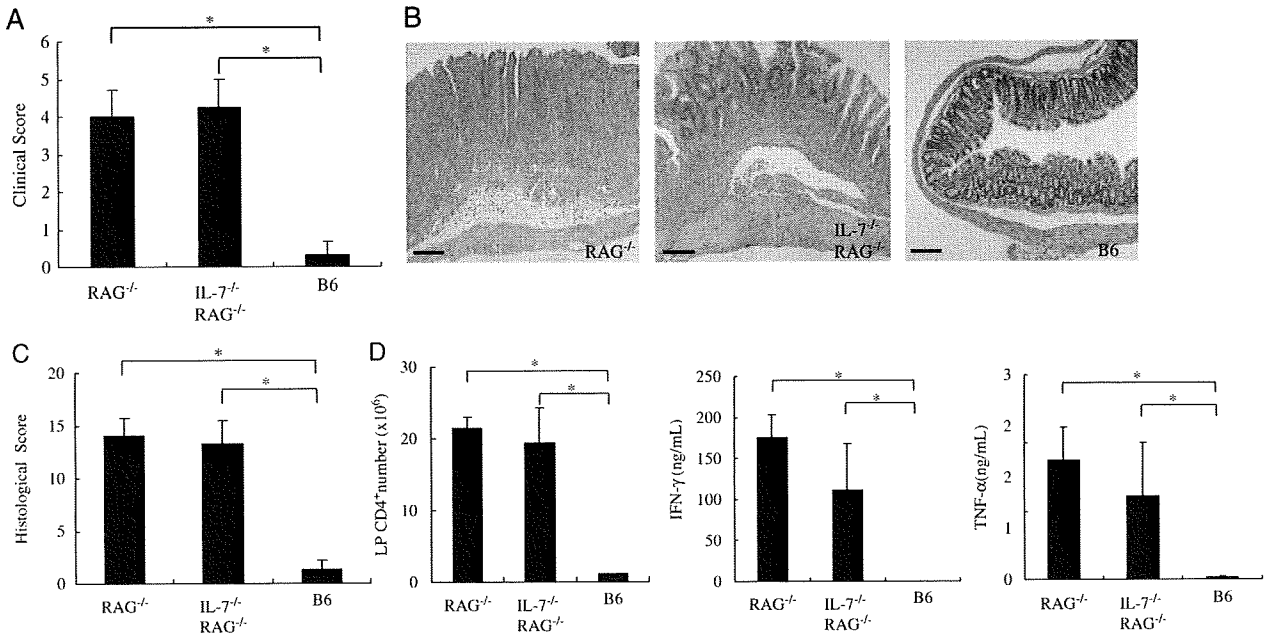

Figure 2. Separated IL-$7^{-/-}$ × RAG-$1^{-/-}$ host mice are consistently diseased after separation. (A) Clinical scores were determined at 12 wk after separation as described in *Materials and methods* and Fig. 1. Data show mean ± SEM (n = 6/group). *p<0.05 *versus* age-matched C57BL/6 mice. (B) Histological examination by H&E staining of the colon. Original magnification, × 100. Bars: 200 μm. (C) Histological scoring of colon. Data show mean ± SEM (n = 6/group). *p<0.01 *versus* control mice. (D) Cell number of $CD4^+$ T cells recovered from LP was determined by flow cytometry. Data show mean ± SEM (n = 6/group). *p<0.01 *versus* control mice. (E) Cytokine production. LP $CD4^+$ T cells were prepared from colons at 12 wk after surgery and stimulated with anti-CD3 and anti-CD28 mAb for 48 h. Concentrations of IFN-γ and TNF-α in culture supernatants were measured by ELISA. Data show mean ± SEM (n = 6/group). *p<0.01, *versus* control C57BL/6 mice.

the persistence of established colitis. Here, by showing that colitis continues in IL-$7^{-/-}$ × RAG-$1^{-/-}$ mice after separation from parabiotic union with colitic RAG-$1^{-/-}$ mice that had previously been transferred with $CD4^+CD45RB^{high}$ T cells. In sharp contrast, we found that IL-7 is essential for the development of on-going colitis under lymphopenic conditions by showing the absence of IL-$7^{-/-}$ × RAG-$1^{-/-}$ mice transferred with colitogenic LP $CD4^+$ T cells obtained from the separated IL-$7^{-/-}$ × RAG-$1^{-/-}$ mice after separation surgery. These results clearly demonstrate that IL-7 is essential for the turnover of colitogenic $CD4^+$ T cells in the lymphopenic stage of the adoptive transfer system, but not for the turnover of those cells in the established stage of colitis in this commensal-dependent adoptive transfer model.

The explanation first considered for the finding that colitic IL-$7^{-/-}$ × RAG-$1^{-/-}$ mice sustained severe colitis up to 12 wk after separation to a similar extent to the paired RAG-$1^{-/-}$ mice was the straightforward migration of IL-7-producing cells or their progenitor cells from RAG-$1^{-/-}$ to IL-$7^{-/-}$ × RAG-$1^{-/-}$ mice in parabionts along with colitogenic $CD4^+$ T cells, since IL-$7^{-/-}$ × RAG-$1^{-/-}$ mice transferred with colitogenic LP $CD4^+$ T cells alone did not develop colitis [26]. However, this possibility was excluded, as RT-PCR analysis could not detect mRNA of IL-7 in the organs or purified $CD45^+CD4^+$ T cells and $CD45^+$ non-T cells of the IL-$7^{-/-}$ × RAG-$1^{-/-}$ mice (Fig. 3A and B), although the possibility remains that IL-7 expressed in the separated IL-$7^{-/-}$ × RAG-$1^{-/-}$ mice at below the level of detection by RT-PCR, contributed to the present result.

Interestingly, however, mRNA expression of IL-15, which has recently been recognized as a homeostatic cytokine for $CD4^+$ memory T cells as well as for the maintenance of $CD8^+$ memory T cells [30–32] was detected at similar levels in various organs of both the separated RAG-$1^{-/-}$ and the IL-$7^{-/-}$ × RAG-$1^{-/-}$ mice (Fig. 3A). However, colitic LP $CD4^+$ T cells in both mice expressed very low levels of IL-15Rβ, an essential receptor for IL-15 signaling, in sharp contrast to the strong expression of IL-7Rα (Fig. 3C). Also, we demonstrated that administration of neutralizing anti-IL-15 mAb did not ameliorate the established colitis in the separated IL-$7^{-/-}$ × RAG-$1^{-/-}$ mice (Fig. 3D). This result suggests that IL-15 is not essential for the sustaining colitis in the separated IL-$7^{-/-}$ × RAG-$1^{-/-}$ mice. Thus, the colitic $CD4^+$ T cells in the parabionts in this study might have acquired a dependency on other cytokines, such as thymic stromal lymphopoietin, receptors of which are composed of IL-7Rα and thymic stromal lymphopoietin, and remained independent of IL-7 during parabiosis. However, this possibility is also unlikely because new IL-$7^{-/-}$ × RAG-$1^{-/-}$ recipients subsequently transferred with colitic LP $CD4^+$ T cells from the separated IL-$7^{-/-}$ × RAG-$1^{-/-}$ mice did not develop colitis (Fig. 4), indicating that IL-7 is essential for the development of on-going colitis in the adoptive transfer system, but not essential for the sustainment of the established chronic colitis after the parabiosis and subsequent separation system.

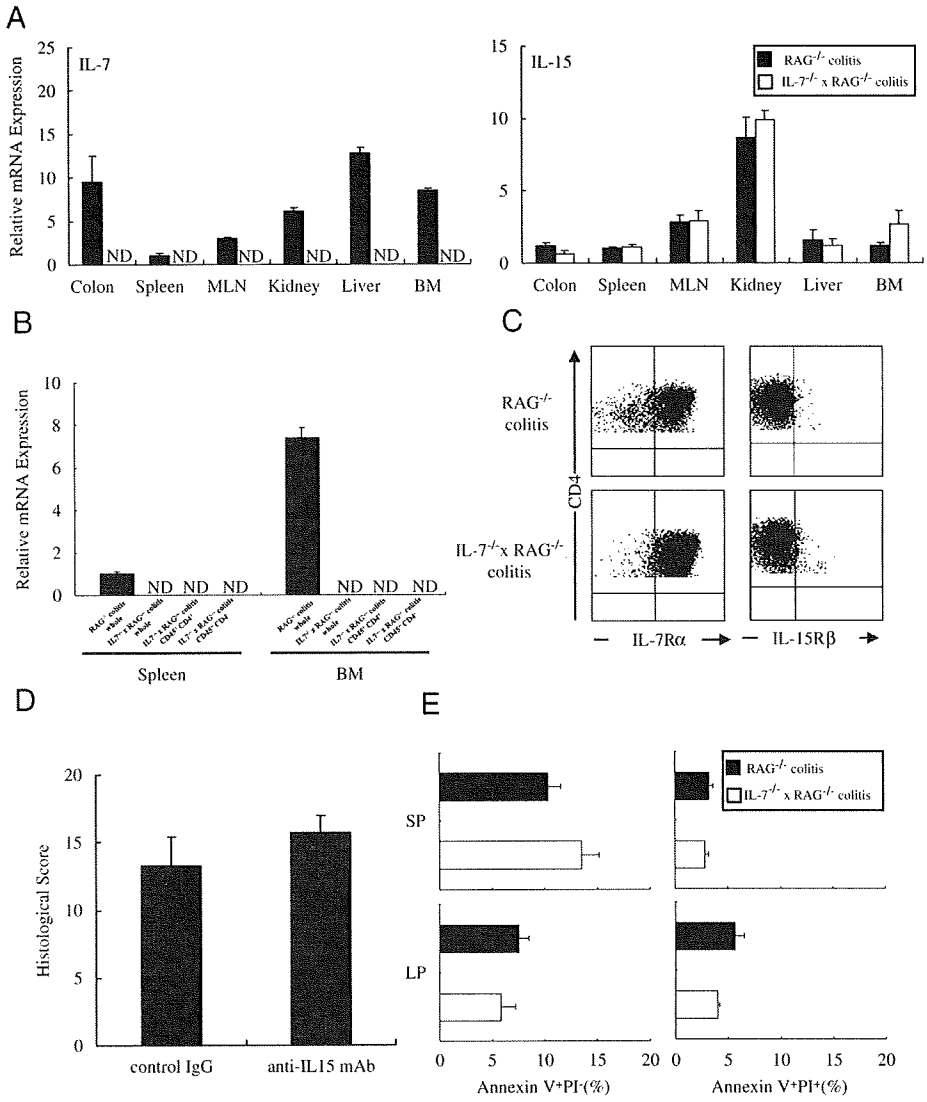

Figure 3. Separated IL-$7^{-/-}$ × RAG-$1^{-/-}$ mice after parabiosis do not express mRNA for IL-7. (A) Expression of IL-7 and IL-15 in mRNA various tissues as determined by real-time RT-PCR. ND, not detected. (B) Expression of IL-7 in various isolated cell populations from spleen and BM. Whole mononuclear cells, $CD45^+$ $CD4^+$ T cells, and $CD45^+$ non-T cells (each 5×10^6 cells) were used for real-time RT-PCR. (C) IL-7Rα and IL-15Rβ expression on LP $CD4^+$ T cells was analyzed by flow cytometry. Data are representive of six mice *per* group. (D) Histological scoring. The separated IL-$7^{-/-}$ × RAG-$1^{-/-}$ mice were administered with anti-IL-15 mAb or control IgG for 6 wk. Data show mean ± SEM (n = 5/group). (E) The ratio of early (Annexin V^+PI^-) and late (Annexin V^+PI^-) apoptotic cells in freshly isolated spleen and LP $CD4^+$ T cells was determined by the Annexin V-FITC/PI. Data show mean ± SEM (n = 5/group). NS, not significantly different.

How can this discrepancy in IL-7 requirement in this adoptive transfer model in combination with parabiosis system be explained? The most striking difference is in the *in vivo* experimental setting, parabiosis *versus* adoptive transfer. In the adoptive transfer system, only a small number of colitogenic $CD4^+$ T cells (approximately 3×10^5–3×10^6 cells/mouse) are transferred into immunodeficient RAG-$1^{-/-}$ mice, whereas in the parabiosis system, a large number of these cells can be continuously transferred into recipients. Thus, it is possible that IL-7 is required for the lymphopenia-driven expansion of these cells in the adoptive transfer system. In contrast, the continuous and abundant supply of these cells in the parabiosis system might overcome the requirement of IL-7 for the development of colitis, this being replaced presumably by other stimuli, such as commensal bacterial antigens and other cytokines. Consistent with this notion, we previously demonstrated that CFSE-labeled colitogenic $CD4^+$ T cells could expand by over eight cell divisions within 7 days after transfer in IL-$7^{-/-}$ × RAG-$1^{-/-}$ mice, a similar extent to that in RAG-$1^{-/-}$ mice, whereas the number of donor-derived cells recovered in IL-$7^{-/-}$ × RAG-$1^{-/-}$ recipients was over 100 times less than that in RAG-$1^{-/-}$ recipients, in line with the decreased expression of Bcl-2 and conversely the increased

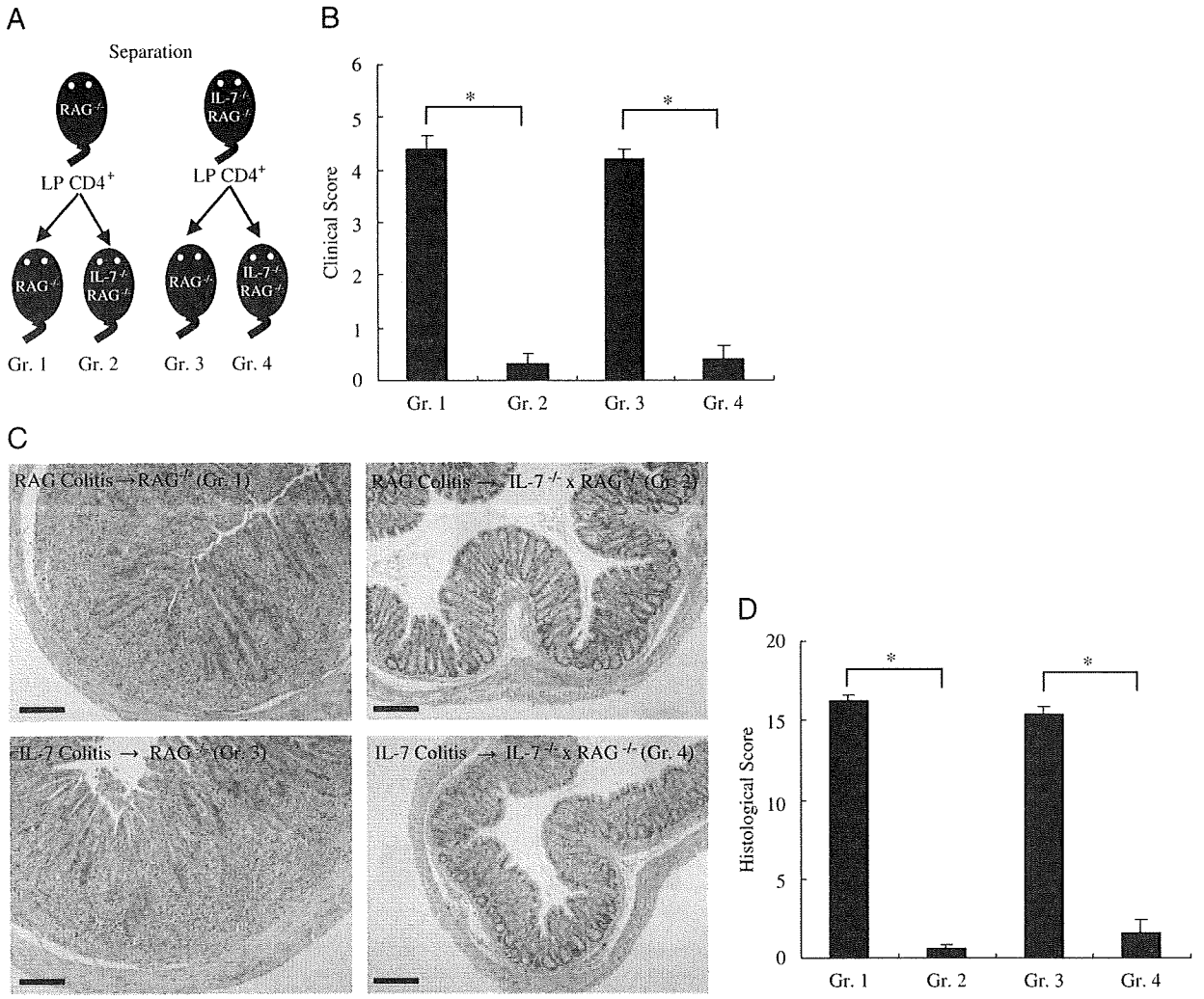

Figure 4. Sustained CD4$^+$ T cells in the separated IL-7$^{-/-}$ × RAG-1$^{-/-}$ *recipients do not have the potential to induce colitis when transferred to new* IL-7$^{-/-}$ × RAG-1$^{-/-}$ *recipients.* (A) New RAG-1$^{-/-}$ or IL-7$^{-/-}$ × RAG-1$^{-/-}$ mice were transferred with LP CD4$^+$ T cells obtained from previously parabiosed RAG-1$^{-/-}$ or IL-7$^{-/-}$ × RAG-1$^{-/-}$ mice at 12 wk after separation (each group; $n = 7$). Group 1 (Gr. 1), new RAG-1$^{-/-}$ mice transferred with LP CD4$^+$ T cells obtained from the separated RAG-1$^{-/-}$ mice; Group 2 (Gr. 2), new RAG-1$^{-/-}$ mice transferred with LP CD4$^+$ T cells from the separated IL-7$^{-/-}$ × RAG-1$^{-/-}$ mice; Group 3 (Gr. 3), new IL-7$^{-/-}$ × RAG-1$^{-/-}$ mice transferred with LP CD4$^+$ T cells from the separated RAG-1$^{-/-}$ mice; Group 4 (Gr. 4), new IL-7$^{-/-}$ × RAG-1$^{-/-}$ mice transferred with LP CD4$^+$ T cells from the separated IL-7$^{-/-}$ × RAG-1$^{-/-}$ mice. (B) Clinical scores were determined 6 wk after transfer. Data show mean ± SEM ($n = 7$/group). *$p<0.01$. (C) Histological examination of the colon. Original magnification, × 100. Bars: 200 μm. (D) Histological scoring. Data show mean ± SEM ($n = 7$/group). *$p<0.01$.

ratio of Annexin V$^+$ apoptotic cells in donor CD4$^+$ T cells of IL-7$^{-/-}$ × RAG-1$^{-/-}$ recipients [26]. Hence, these results suggest that IL-7 is indeed not required for rapid proliferation of colitogenic LP CD4$^+$ T cells in lymphopenic conditions, but is concurrently critical for the survival of those cells until the time that recipient mice become lympho-competent.

The current findings might also shed light on the clinical aspect of IBD. Most current treatments for IBD, such as corticosteroid, immunosuppresants (azathiopurine and cyclosporine), and biologics (infliximab), induce apoptosis of activated CD4$^+$ T cells [33], and thereby are often accompanied by lymphopenia. This is also the case with the recently developed therapy by autologous hematopoietic stem cell transplantation for patients with intractable Crohn's disease [34]. However, since most patients who achieve remission by these treatments inevitably relapse some time later, it is possible that subsequent blockade of the IL-7/IL-7R signal pathway to suppress IL-7-dependent lymphopenia-driven expansion of colitogenic CD4$^+$ T cells will be beneficial for the long-term remission of the diseases.

In summary, we here demonstrated that IL-7 is essential for the turnover of colitogenic CD4$^+$ T cells in the lymphopenic stage of colitis in the commensal-dependent adoptive transfer model, suggesting an effectual timing for therapeutic approaches that target systemic IL-7 using the biologics against IL-7 in the treatment of IBD.

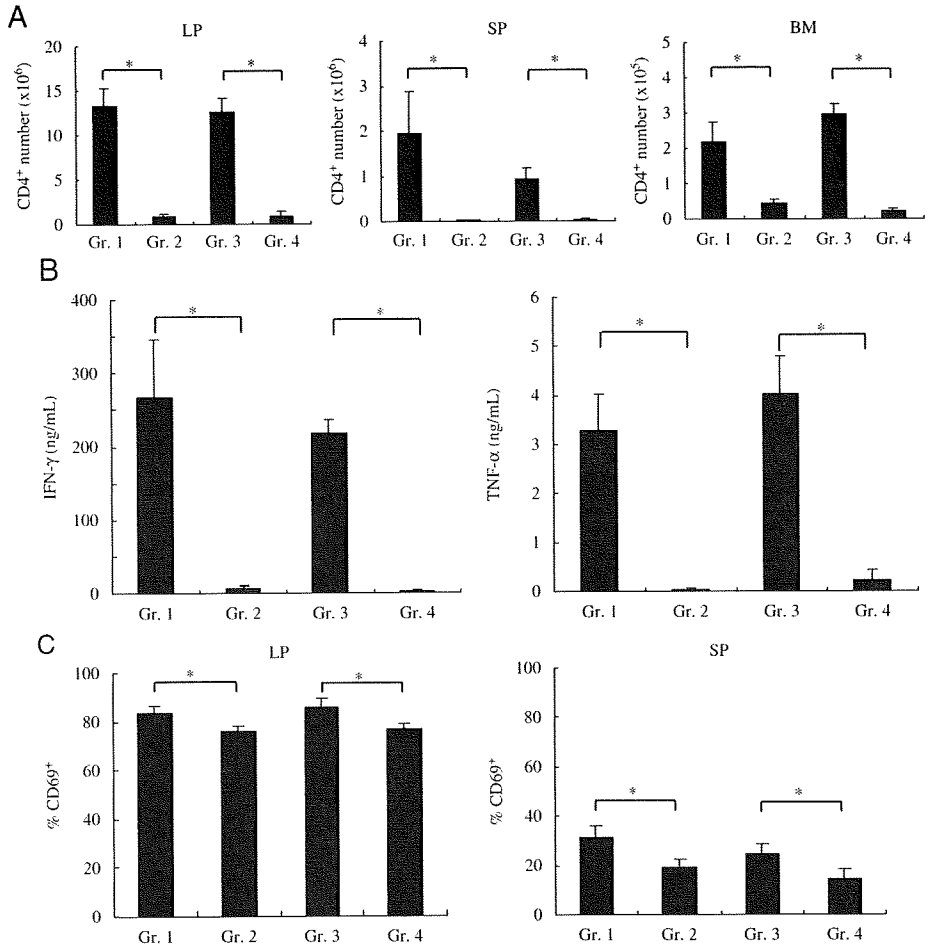

Figure 5. Adoptive transfer of sustained $CD4^+$ T cells in the separated IL-$7^{-/-}$ × RAG-$1^{-/-}$ *recipients into* IL-$7^{+/+}$ × RAG-$1^{-/-}$, *but not* IL-$7^{-/-}$ × RAG-$1^{-/-}$, *recipients induce Th1-mediated colitis.* Group 1 (Gr. 1)–Group 4 (Gr. 4); see Fig. 4. (A) Cells were isolated from LP, SP, and BM, and the number of $CD4^+$ cells was determined by flow cytometry. (B) Cytokine production by LP $CD4^+$ T cells. $CD4^+$ were isolated from each mouse at 6 wk after transfer and stimulated with anti-CD3 and anti-CD28 mAb for 48 h. IFN-γ and TNF-α concentrations in culture supernatants were measured by ELISA. (C) Expression of CD69 on LP and SP $CD4^+$ T cells from each group. Data show mean ± SEM ($n = 7$/group). *$p<0.05$.

Materials and methods

Animals

C57BL/6-Ly5.2 mice were purchased from Japan Clea (Tokyo, Japan). C57BL/6-Ly5.2-RAG-2-deficient (RAG-$2^{-/-}$) were obtained from Taconic Laboratory (Hudson, NY, USA) and Central Laboratories for Experimental Animals (Kawasaki, Japan). C57BL/6-Ly5.2-background RAG-$1^{+/-}$ and IL-$7^{+/-}$ mice were kindly provided by Dr. R. Zamoyska (National Institute for Medical Research) and Dr. P. Vieira (Institut Pasteur) [16, 35]. These mice were intercrossed to generate IL-$7^{-/-}$ × RAG-$1^{-/-}$ and IL-$7^{+/+}$ × RAG-$1^{-/-}$ (hereafter RAG-$1^{-/-}$) littermate mice in the Animal Care Facility of Tokyo Medical and Dental University. Mice were maintained under specific pathogen-free conditions in the Animal Care Facility of Tokyo Medical and Dental University. Donors and recipients were used at 6–12 wk of age. All experiments were approved by the regional animal study committees and were performed according to institutional guidelines and Home Office regulations.

Parabiosis

We performed an adoptive transfer experiment in combination with a parabiosis system using RAG-$1^{-/-}$ and IL-$7^{-/-}$ × RAG-$1^{-/-}$ littermate recipients (Fig. 1A). For the adoptive transfer, $CD4^+$ T cells were first isolated from spleen cells of C57BL/6-Ly5.2 mice using the anti-CD4 (L3T4)-MACS system (Miltenyi Biotec, Auburn, CA, USA) according to the manufacturer's instructions. Enriched $CD4^+$ T cells (96–97% pure, as estimated by FACS Calibur (Becton Dickinson, Sunnyvale, CA,

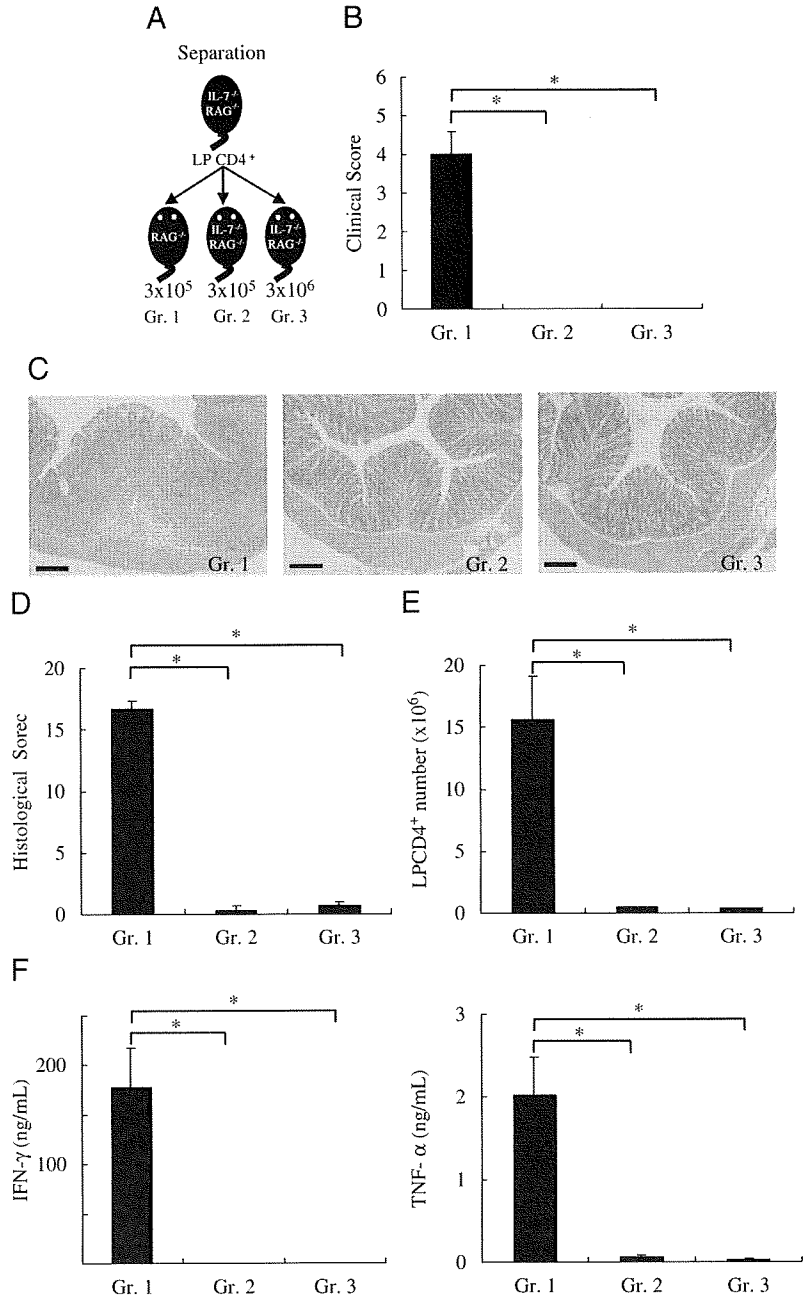

Figure 6. Adoptive transfer of a large number of sustained $CD4^+$ T cells in the separated IL-$7^{-/-}$ × RAG-$1^{-/-}$ recipients into IL-$7^{-/-}$ × RAG-$1^{-/-}$ recipients does not induce colitis. (A) New RAG-$1^{-/-}$ or IL-$7^{-/-}$ × RAG-$1^{-/-}$ mice transferred with LP $CD4^+$ T cells (3×10^5–3×10^6) were obtained from previously parabiosed IL-$7^{-/-}$ × RAG-$1^{-/-}$ mice at 12 wk after separation surgery (each group; $n = 5$). (B) Clinical scores were determined 12 wk after transfer. Data show mean ± SEM ($n = 7$/group). *$p<0.01$. (C) Histological examination of the colon. Original magnification, × 100. Bars: 200 μm. (D) Histological scoring. Data show mean ± SEM ($n = 7$/group). *$p<0.01$. (E) The number of LP $CD4^+$ cells was determined by flow cytometry. Data show mean ± SEM ($n = 7$/group). *$p<0.05$. (F) Cytokine production by LP $CD4^+$ T cells. $CD4^+$ were isolated from each mouse at 12 wk after transfer and stimulated with anti-CD3 and anti-CD28 mAb for 48 h. IFN-γ and TNF-α concentrations in culture supernatants were measured by ELISA. Data show mean ± SEM ($n = 7$/group). *$p<0.05$.

USA) were then labeled with PE-conjugated anti-mouse CD4 (RM4-5; BD PharMingen, San Diego, CA, USA) and FITC-conjugated anti-CD45RB (16A; BD PharMingen). $CD4^+$ $CD45RB^{high}$ cells were generated using a FACS Aria (Becton Dickinson). This population was >98.0% pure on reanalysis. RAG-$1^{-/-}$ mice ($n = 12$) were then injected intraperitoneally with 3×10^5 splenic $CD4^+CD45RB^{high}$ T cells from normal C57BL/6-Ly5.2 mice. At 6 wk after transfer, RAG-$1^{-/-}$ mice

transferred with $CD4^+CD45RB^{high}$ T cells developed a wasting disease and colitis as reported previously [26]. We then carried out parabiosis surgery [28] according to institutional guidelines and Home Office regulations. Briefly, sex-matched mice were anesthetized prior to surgery, and incisions were made in the skin on the opposing flanks of the donor and recipient animals. Surgical sutures were used to bring the body walls of the two mice into direct physical contact. The outer skin was then attached with surgical staples. In this way, colitic RAG-$1^{-/-}$ mice that had previously been transferred with $CD4^+CD45RB^{high}$ T cells were parabiosed with new IL-$7^{-/-}$ × RAG-$1^{-/-}$ mice ($n = 12$). All parabionts were observed for clinical signs such as hunched posture, piloerection, diarrhea, and blood in the stool. At autopsy, mice were assessed for a clinical score as described previously [36].

Adoptive transfer experiment after separation of parabionts

To further investigate the role of IL-7 in the maintenance of colitogenic $CD4^+$ memory T cells, we next separated the parabionts surgically at 6 wk after theparabiosis surgery. All mice were observed for clinical signs for 12 wk after separation, and assessed for a clinical score at autopsy as described above [36]. To assess the possibility that some colitogenic $CD4^+$ T cells acquired IL-7-independency during parabiosis or after separation, LP $CD4^+$ T cells (3×10^5 or 3×10^6 cells) isolated from the separated RAG-$1^{-/-}$ or IL-$7^{-/-}$ × RAG-$1^{-/-}$ mice were transferred into new RAG-$1^{-/-}$ or IL-$7^{-/-}$ × RAG-$1^{-/-}$ mice. All mice were observed for clinical signs for 6 or 12 wk after transfer. In another set of experiments, the separated IL-$7^{-/-}$ × RAG-$1^{-/-}$ mice were i.p. administered with 250 μg of neutralizing anti-IL-15 mAb (AIO.3) [37] or control rat IgG (Sigma, St. Louis, MO, USA) in 250 μL PBS every week over a period of 6 wk. All mice were observed for clinical signs for 6 wk after separation.

Histological examination

Tissue samples were fixed in PBS containing 10% neutral-buffered formalin. Paraffin-embedded sections (5 μm) were stained with H&E. Three tissue samples from the proximal, middle, and distal parts of the colon were prepared. The sections were analyzed without prior knowledge of the type of T-cell reconstitution or treatment. The area most affected was graded by the number and severity of lesions. The mean degree of inflammation in the colon was calculated using a modification of a previously described scoring system [38].

Tissue preparations

Single cell suspensions were prepared from spleen, LP, and BM as described previously [39]. To isolate LP $CD4^+$ T cells, the entire length of colon was opened longitudinally, washed with PBS, and cut into small pieces. The dissected mucosa was incubated with Ca^{2+}, Mg^{2+}-free Hanks' BSS containing 1 mM DTT (Sigma-Aldrich) for 45 min to remove mucus and then treated with 3.0 mg/mL collagenase (Roche Diagnosyics GmbH, Germany) and 0.01% DNase (Worthington Biomedical, Freehold, NJ, USA) for 2 h. The cells were pelleted two times through a 40% isotonic Percoll solution, and then subjected to Ficoll–Hypaque density gradient centrifugation (40/75%). Enriched LP $CD4^+$ T cells were obtained by positive selection using anti-CD4 (L3T4) MACS magnetic beads. The resultant cells when analyzed by FACS Calibur contained >95% $CD4^+$ cells. BM cells were obtained by flushing two femurs with cold RPMI 1640.

Real-time RT-PCR

Total RNA was isolated by using ISOGEN reagent (NIPPON GENE). Aliquots of 0.5 μg of total RNA were used for complementary DNA synthesis in 20 μL of reaction volume by using random primers. To validate gene expression changes, quantitative RT-PCR analysis was performed by Applied Biosystems 7500 using validated TaqMan Gene Expression Assays (Applied Biosystems). The TaqMan probes and primers for mouse IL-7 (assay identification number Mm01295805_m1) and mouse IL-15 (assay identification number Mm00434210_m1) were Assay-on-Demand gene expression products (Applied Biosystems). The mouse β-actin gene was used as endogenous control (catalog number 4352933E; Applied Biosystems). The thermal cycler conditions were as follows: hold for 10 min at 95°C, followed a cycle of 95°C for 15 s and 60°C for 1 min for 50 cycles. All samples were treated in triplicate. Amplification data were analyzed with an Applied Biosystems Sequence Detection Software version 1.3, and the relative mRNA amounts and range were determined. Briefly, we normalized each set of samples using the difference in threshold cycles (ΔCT) between the sample gene and housekeeping gene (β-actin):ΔCT = (ΔCtsample−ΔCTβ-actin). The calibrator sample (ΔCTcalibration) was assigned as the sample with the RAG-$2^{-/-}$ colitic mice in each set. Relative mRNA levels were calculated by the expression $2^{-\Delta\Delta CT}$ where ΔΔCT = ΔCtsample (n) −ΔCtcalibration (n).

Cytokine ELISA

To measure cytokine production, 1×10^5 LP $CD4^+$ T cells were cultured in 200 μL of culture medium at 37°C in a humidified atmosphere containing 5% CO_2 in 96-well plates (Costar, Cambridge, MA, USA) pre-coated with 5 μg/mL hamster anti-mouse CD3ε mAb (145-2C11, BD PharMingen) and hamster 2 μg/mL anti-mouse CD28 mAb (37.51, BD PharMingen) in PBS overnight at 4°C. Culture supernatants were removed after 48 h and assayed for cytokine production. Cytokine concentrations were determined by specific ELISA as *per* the manufacturer's recommendation (R&D, Minneapolis, MN, USA).

Flow cytometry

To detect the surface expression of a variety of molecules, isolated splenocytes, BM, or LP mononuclear cells were preincubated with an FcγR-blocking mAb (CD16/32; 2.4G2, BD PharMingen) for 15 min followed by incubation with specific FITC-, PE-, PerCP-, allophycocyanin-, or biotin-labeled antibodies for 20 min on ice. The following mAb were obtained from BD PharMingen: anti- CD4 mAb (RM4-5), anti-CD45RB mAb (16A), anti-CD69 mAb (H1.2F3), anti-IL-7Rα mAb (A7R34), anti-CD44 mAb (IM7), anti-IL-15Rβ (5H4) and anti-CD62L mAb (MEL-14). Standard two-, three-, or four-color flow cytometric analyses were obtained using the FACS Calibur using CellQuest software. Background fluorescence was assessed by staining with control irrelevant isotype-matched mAb.

Statistical analysis

The results were expressed as the mean ± standard error of mean (SEM). Groups of data were compared by Mann–Whitney *U*-test. Differences were considered to be statistically significant when $p<0.05$.

Acknowledgements: The authors are grateful to Zamoyska R for providing mice. They thank T. Fujii and O. Yamaji for technical assistance. This study was supported in part by grants-in-aid for Scientific Research, Scientific Research on Priority Areas, Exploratory Research and Creative Scientific Research from the Japanese Ministry of Education, Culture, Sports, Science and Technology; the Japanese Ministry of Health, Labor and Welfare; the Japan Medical Association; Medical School Faculty and Alumni Grants of Keio University Medical Science Fund; Foundation for Advancement of International Science; Terumo Life Science Foundation; Ohyama Health Foundation; Yakult Bio-Science Foundation; Research Fund of Mitsukoshi Health and Welfare Foundation.

Conflict of interest: The authors declare no financial or commercial conflict of interest.

Reference

1 Podolsky, D. K., Inflammatory bowel disease. *N. Engl. J. Med.* 2002. **347**: 417–429.

2 Sands, B. E., Inflammatory bowel disease: past, present, and future. *J. Gastroteol.* 2007. **42**: 16–25.

3 Strober, W., Fuss, I. J. and Blumberg, R. S., The immunology of mucosal models of inflammation. *Annu. Rev. Immunol.* 2002. **20**: 495–549.

4 Bamias, G., Nyce, M. R., De La Rue, S. A. and Cominelli, F., New concepts in the pathophysiology of inflammatory bowel disease. *Ann. Intern. Med.* 2005. **143**: 895–904.

5 Sartor, R. B., Mechanisms of disease: pathogenesis of Crohn's disease and ulcerative colitis. *Nat. Clin. Pract. Gastroenterol. Hepatol.* 2006. **3**: 390–407.

6 Hibi, T. and Ogata, H., Novel pathophysiological concepts of inflammatory bowel disease. *J. Gastroteol.* 2006. **41**: 10–16.

7 Baumgart, D. C. and Sandborn, W. J., Inflammatory bowel disease: clinical aspects and established and evolving therapies. *Lancet* 2007. **369**: 1641–1657.

8 Zhang, Y., Joe, G., Hexner, E., Zhu, J. and Emerson, S. G., Host-reactive CD8+memory stem cells in graft-*versus*-host disease. *Nat. Med.* 2005. **11**: 1299–1305.

9 Jameson, S. C., Maintaining the norm: T-cell homeostasis. *Nat. Rev. Immunol.* 2002. **2**: 547–556.

10 Seder, R. A. and Ahmed, R., Similarities and differences in $CD4^+$ and $CD8^+$ effector and memory T cell generation. *Nat. Immunool.* 2003. **4**: 835–842.

11 Harty, J. T. and Badovinac, V. P., Shaping and reshaping $CD8^+$ T-cell memory. *Nat. Rev. Immunol.* 2008. **8**: 107–119.

12 Schluns, K. S. and Lefrancois, L., Cytokine control of memory T-cell development and survival. *Nat. Rev. Immunol.* 2003. **3**: 269–279.

13 Ma, A., Koka, R. and Burkett, P., Diverse functions of IL-2, IL-15, and IL-7 in lymphoid homeostasis. *Annu. Rev. Immunol.* 2006. **24**: 657–679.

14 Bradley, L. M., Haynes, L. and Swain, S. L., IL-7: maintaining T-cell memory and achieving homeostasis. *Trends Immunol.* 2005. **26**: 172–176.

15 Klenerman, P. and Hill, A., T cells and viral persistence: lessons from diverse infections. *Nat. Immunol.* 2005. **6**: 873–879.

16 Seddon, B., Tomlinson, P. and Zamoyska, R., Interleukin 7 and T cell receptor signals regulate homeostasis of CD4 memory cells. *Nat. Immunol.* 2003. **4**: 680–686.

17 Robertson, J. M., MacLeod, M., Marsden, V. S., Kappler, J. W. and Marrack, P., Not all $CD4^+$ memory T cells are long lived. *Immunol. Rev.* 2006. **211**: 49–57.

18 Barber, D. L., Wherry, E. J., Masopust, D., Zhu, B., Allison, J. P., Sharpe, A. H., Freeman, G. J. and Ahmed, R., Restoring function in exhausted CD8 T cells during chronic viral infection. *Nature* 2006. **439**: 682–687.

19 Sharpe, A. H., Wherry, E. J., Ahmed, R. and Freeman, G. J., The function of programmed cell death 1 and its ligands in regulating autoimmunity and infection. *Nat. Immunol.* 2007. **8**: 239–245.

20 Maloy, K. and Powrie, F., Regulatory T cells in the control of immune pathology. *Nat. Immunol.* 2001. **2**: 816–822.

21 Namen, A. E., Lupton, S., Hjerrild, K., Wignall, J., Mochizuki, D. Y., Schmierer, A., Mosley, B. *et al.*, Stimulation of B-cell progenitors by cloned murine interleukin-7. *Nature* 1988. **333**: 571–573.

22 Watanabe, M., Uen, Y., Yajima, T., Iwao, Y., Tsuchiya, M., Ishikawa, H., Aiso, S. *et al.*, Interleukin 7 is produced by human intestinal epithelial cells and regulates the proliferation of intestinal mucosal lymphocytes. *J. Clin. Invest.* 1995. **95**: 2945–2953.

23 Fry, T. J. and Mackall, C. L., The many faces of IL-7: from lymphopoiesis to peripheral T-cell maintenance. *J. Immunol.* 2005. **174**: 6571–6576.

24 Watanabe, M., Ueno, Y., Yajima, T., Okamoto, S., Hayashi, T., Yamazaki, M., Iwao, Y. *et al.*, Interleukin 7 transgenic mice develop chronic colitis with decreased interleukin 7 protein accumulation in the colonic mucosa. *J. Exp. Med.* 1998. **187**: 389–402.

25 Yamazaki, M., Yajima, T., Tanabe, M., Fukui, K., Okada, E., Okamoto, R., Oshima, S. *et al.*, Mucosal T cells expressing high levels of IL-7 receptor are potential targets for treatment of chronic colitis. *J. Immunol.* 2003. **171**: 1556–1563.

26 **Totsuka, T., Kanai, T., Nemoto, Y., Makita, S. and Watanabe, M.,** IL-7 is essential for the development and the persistence of chronic colitis. *J. Immunol.* 2007. **178**: 4737–4748.

27 **Powrie, F., Leach, M. W., Mauze, S., Caddle, L. B. and Coffman, R. L.,** Phenotypically distinct subsets of $CD4^+$ T cells induce or protect from chronic intestinal inflammation in C.B-17 scid mice. *Int. Immunol.* 1993. **5**: 1461–1471.

28 **Tomita, T., Kanai, T., Nemoto, Y., Totsuka, T., Okamoto, R., Tsuchiya, K., Sakamoto, N. and Watanabe, M.,** Systemic, but not intestinal, IL-7 is essential for the persistence of chronic colitis. *J. Immunol.* 2008. **180**: 383–390.

29 **Dereuddre-Bosquet, N., Vaslin, B., Delache, B., Brochard, P., Clayette, P., Aubenque, C., Morre, M. *et al.*,** Rapid modifications of peripheral T-cell subsets that express CD127 in macaques treated with recombinant IL-7. *J. Med. Primatol.* 2007. **36**: 228–237.

30 **Picker, L. J., Reed-Inderbitzin, E. F., Hagen, S. I., Edgar, J. B., Hansen, S. G., Legasse, A., Planer, S. *et al.*,** IL-15 induces CD4 effector memory T cell production and tissue emigration in nonhuman primates. *J. Clin. Invest.* 2006. **116**: 1514–1524.

31 **Purton, J. F, Tan, J. T., Rubinstein, M. P., Kim, D. M., Sprent, J. and Surh, C. D.,** Antiviral $CD4^+$ memory T cells are IL-15 dependent. *J. Exp. Med.* 2007. **204**: 951–961.

32 **Zeng, R., Spolski, R., Finkelstein, S. E., Oh, S., Kovanen, P. E., Hinrichs, C. S., Pise-Masison, C. A. *et al.*,** Synergy of IL-21 and IL-15 in regulating CD8+T cell expansion and function. *J. Exp. Med.* 2005. **201**: 139–148.

33 **Sartor, R. B.,** Therapeutic manipulation of the enteric microflora in inflammatory bowel diseases: antibiotics, probiotics, and prebiotics. *Gastroenterology* 2004. **126**: 1620–1633.

34 **Oyama, Y., Craig, R. M., Traynor, A. E., Quigley, K., Statkute, L., Halverson, A., Brush, M. *et al.*,** Autologous hematopoietic stem cell transplantation in patients with refractory Crohn's disease. *Gastroenterology* 2005. **128**: 552–563.

35 **von Freeden-Jeffry, U., Vieira, P., Lucian, L. A., McNeil, T., Burdach, S. E. and Murray, R.,** Lymphopenia in interleukin (IL)-7 gene-deleted mice identifies IL-7 as a nonredundant cytokine. *J. Exp. Med.* 1995. **181**: 1519–1526.

36 **Totsuka, T., Kanai, T., Iiyama, R., Uraushihara, K., Yamazaki, M., Okamoto, R., Hibi, T. *et al.*,** Ameliorating effect of anti-ICOS monoclonal antibody in a murine model of chronic colitis. *Gastroenterology* 2003. **124**: 410–421.

37 **Ohteki, T., Tada, H., Ishida, K., Sato, T., Maki, C., Yamada, T., Hamuro, J. and Koyasu, S.,** Essential roles of DC-derived IL-15 as a mediator of inflammatory responses *in vivo*. *J. Exp. Med.* 2006. **203**: 2329–2338.

38 **Makita, S., Kanai, T., Nemoto, Y., Totsuka, T., Okamoto, R., Tsuchiya, K., Yamamoto, M. *et al.*,** Intestinal lamina propria retaining $CD4^+CD25^+$ regulatory T cells is a suppressive site of intestinal inflammation. *J. Immunol.* 2007. **178**: 4937–4946.

39 **Nemoto, Y., Kanai, T., Makita, S., Okamoto, R., Totsuka, T., Takeda, K. and Watanabe, M.,** Bone marrow retaining colitogenic $CD4^+$ T cells may be a pathogenic reservoir for chronic colitis. *Gastroenterology* 2007. **132**: 176–189.

Abbreviations: **IBD:** inflammatory bowel diseases · **LP:** lamina propria

Full correspondence: Dr. Takanori Kanai, Department of Gastroenterology and Hepatology, Keio University School of Medicine, 35 Shinanomachi Shinjuku-ku, Tokyo 160–8582, Japan
Fax: +81-3-3341-3631
e-mail: takagast@sc.itc.keio.ac.jp

Received: 11/9/2008
Revised: 11/6/2009
Accepted: 14/7/2009

Am J Physiol Gastrointest Liver Physiol 296: G23–G35, 2009.
First published November 20, 2008; doi:10.1152/ajpgi.90225.2008.

Requirement of Notch activation during regeneration of the intestinal epithelia

Ryuichi Okamoto,[1,2] Kiichiro Tsuchiya,[2] Yasuhiro Nemoto,[2] Junko Akiyama,[2] Tetsuya Nakamura,[1,2] Takanori Kanai,[2] and Mamoru Watanabe[2]

[1]*Department of Advanced Therapeutics in Gastrointestinal Diseases and* [2]*Department of Gastroenterology and Hepatology, Graduate School, Tokyo Medical and Dental University, Tokyo, Japan*

Submitted 7 March 2008; accepted in final form 18 November 2008

Okamoto R, Tsuchiya K, Nemoto Y, Akiyama J, Nakamura T, Kanai T, Watanabe M. Requirement of Notch activation during regeneration of the intestinal epithelia. *Am J Physiol Gastrointest Liver Physiol* 296: G23–G35, 2009. First published November 20, 2008; doi:10.1152/ajpgi.90225.2008.—Notch signaling regulates cell differentiation and proliferation, contributing to the maintenance of diverse tissues including the intestinal epithelia. However, its role in tissue regeneration is less understood. Here, we show that Notch signaling is activated in a greater number of intestinal epithelial cells in the inflamed mucosa of colitis. Inhibition of Notch activation in vivo using a γ-secretase inhibitor resulted in a severe exacerbation of the colitis attributable to the loss of the regenerative response within the epithelial layer. Activation of Notch supported epithelial regeneration by suppressing goblet cell differentiation, but it also promoted cell proliferation, as shown in in vivo and in vitro studies. By utilizing tetracycline-dependent gene expression and microarray analysis, we identified a novel group of genes that are regulated downstream of Notch1 within intestinal epithelial cells, including PLA2G2A, an antimicrobial peptide secreted by Paneth cells. Finally, we show that these functions of activated Notch1 are present in the mucosa of ulcerative colitis, mediating cell proliferation, goblet cell depletion, and ectopic expression of PLA2G2A, thereby contributing to the regeneration of the damaged epithelia. This study showed the critical involvement of Notch signaling during intestinal tissue regeneration, regulating differentiation, proliferation, and antimicrobial response of the epithelial cells. Thus Notch signaling is a key intracellular molecular pathway for the proper reconstruction of the intestinal epithelia.

intestinal epithelial cells; goblet cells; PLA2G2A; ulcerative colitis

THE INTESTINAL EPITHELIA are composed of four lineages of intestinal epithelial cells (IECs) that arise from intestinal stem cells (1). Recent studies have shown that various signals such as Wnt, Sonic hedgehog, and bone morphogenetic protein interact within the stem and progenitor cells of the intestinal epithelia to finely regulate the expansion and the cell fate decision of IECs. Other studies have revealed that Notch signaling may also play critical roles in the maintenance of the intestinal epithelia (20).

Notch signaling is a signaling pathway known to regulate differentiation and proliferation of cells in diverse adult tissues (1). Activation of Notch receptor is mediated by the cleavage of its intracellular domain (NICD), and this intracellular domain translocates from the cell membrane to the nucleus, thereby functioning as a transcriptional activator of target genes such as Hes1 (10, 25). The functional role of Notch signaling in the intestine was first described in a study of Hes1-null mice; depletion of Hes1 was associated with significant increases in the secretory lineage IECs (9). Other studies have shown that the activation of Notch promoted proliferation of crypt progenitor cells and directed their cell fates toward absorptive but not secretory lineage cells (6, 28, 33). A recent study suggested that Notch might also function in postmitotic IECs, directing their cell fates toward secretory lineage cells (42). Thus these studies have suggested that Notch signaling functions in the intestine to regulate differentiation and proliferation of IECs, contributing to the maintenance and the homeostasis of the intestinal mucosa. However, the role of Notch signaling in tissue regeneration is less understood.

Damage of the intestinal epithelia is observed in a wide variety of diseases, such as acute intestinal infections, radiation injuries, or idiopathic inflammatory bowel diseases (23). Once the epithelial layer is damaged, it responds by restoring the continuity and integrated structure via activating the stepwise regeneration program (16). The initial response is called restitution, which is the redistribution of remaining IECs to rapidly cover the damaged area. This initial step is usually completed in an extremely short period of time and thus does not require the proliferation or expansion of IECs (19). However, in the next step, the rapid expansion of IECs is necessary to rebuild the proper structure of the epithelia. This response is manifested by the appearance of the regenerative epithelia in the intestine, showing a marked expansion of the proliferating compartment consisting of undifferentiated IECs. However, the exact molecular mechanisms involved in this critical step of intestinal epithelial regeneration has never been described.

Another change that is observed in the intestine during such a regenerative process is the ectopic expression of antimicrobial peptides by IECs. Paneth cells usually secrete peptides such as lysozymes, α-defensins, or PLA2G2A, and this helps to maintain the ideal environment for the stem and progenitor IECs within the small intestinal crypts. The ectopic expressions of these antimicrobial peptides by IECs are frequently observed in the inflamed colonic mucosa (5, 8), and such expressions likely support the local immune system in providing an ideal environment for the regeneration of the damaged mucosa.

In this study, we show that Notch signaling is activated in many IECs in the inflamed mucosa of murine colitis. Results show that the activation of Notch is critical for the proper regeneration program in the epithelial layer and that it helps to suppress goblet cell differentiation and promote cell proliferation. A comprehensive analysis identified a novel group of genes regulated by Notch in IECs, which included

Address for reprint requests and other correspondence: M. Watanabe, Dept. of Gastroenterology and Hepatology, Graduate School, Tokyo Medical and Dental Univ., 1-5-45 Yushima, Bunkyo-ku, Tokyo 113-8519, Japan (e-mail address: mamoru.gast@tmd.ac.jp).

The costs of publication of this article were defrayed in part by the payment of page charges. The article must therefore be hereby marked "*advertisement*" in accordance with 18 U.S.C. Section 1734 solely to indicate this fact.

a gene encoding an antimicrobial peptide called PLA2G2A. Such functions of Notch activation were present not only in the mice intestine but also in the human intestine. Finally, the clinical relevance of Notch-mediated regeneration is analyzed in ulcerative colitis (UC). Thus Notch signaling is a key-signaling pathway involved in intestinal tissue regeneration, in fine regulation of differentiation and proliferation, and in antimicrobial activities in IECs. Our findings point to a novel molecular target for agents that could promptly regenerate the intestinal mucosa in a wide range of intestinal diseases.

MATERIALS AND METHODS

Mice. C57BL/6J mice at 8 wk of age were purchased from Japan Clea. Mice were housed and maintained in the animal facility of Tokyo Medical and Dental University. The institutional animal use and care committee approved the study.

In vivo experiments. Induction of colitis was performed as previously described (17). Briefly, mice were fed ad libitum with 1.75% dextran sodium sulfate (DSS, Bio Research of Yokohama) for 5 consecutive days, followed by distilled water for another 5 days. For inhibition of Notch activation, mice were orally administered with either 5% DMSO (vehicle, VEC) or LY411,575 (LY) (10 mg/kg) dissolved in 0.5% (wt/vol) methylcellulose (WAKO), once daily for 5 consecutive days. Twenty-four mice were separated into four groups: *1*) fed distilled water for five days followed by daily administration of vehicle alone (VEC, $n = 6$) for 5 days, *2*) fed distilled water for 5 days followed by daily administration of LY411,575 (LY, $n = 6$) for five days, *3*) fed 1.75% DSS for 5 days followed by daily administration of vehicle (DSS + VEC, $n = 6$) for 5 days, and *4*) fed 1.75% DSS for 5 days followed by daily administration of LY411,575 (DSS + LY, $n = 6$) for 5 days. The whole body weights of mice were measured everyday. They were euthanized 12 h after the final administration. Colonic tissues were subjected to hematoxylin and eosin staining and analyzed by histological scoring following the criteria described elsewhere (21). Flow cytometry of thymocytes and splenocytes were performed as previously described (35, 41).

Immunoblot analysis. Immunoblots were performed as described elsewhere (18). The primary antibodies used were anti-Cleaved Notch1 (1:1,000, Cell Signaling Technology), anti-Hes1 (1:4,000, a kind gift from Dr. T. Sudo), and anti-β-actin (1:5,000, Sigma). Proteins were visualized either by the ECL Advance Western Blotting Kit (GE Healthcare) or ECL Western Blotting Kit (GE Healthcare).

Cell culture. The cell cultures and transfections of plasmid DNA were performed as described elsewhere (18). The inhibition of Notch signaling was achieved by the addition of LY411,575 (1 μM), synthesized according to Wu et al. (38). A cell line expressing Notch1 intracellular domain (Tet-On NICD1 cells) under the control of tetracycline or doxycycline (DOX, 100 ng/ml, Clontech) was generated as described elsewhere (18), using LS174T cells as parent cells. The cell lines were supplemented with Blastcidin (7.5 μg/ml, Invitrogen) and Zeocin (750 μg/ml, Invitrogen) for their maintenance.

RT-PCR assays. RT-PCR was performed as described elsewhere (18). Quantitative analyses using the SYBR green master mix (Qiagen) was performed by ABI 7500 (Applied Biosystems). Primer sequences for human β-actin, G3PDH, or MUC2 have been previously described (30). The primer sequences for other genes are summarized in Table 1. The results are shown as the means of the data collected from two rounds of assays, with each assay performed in triplicate. The data were statistically analyzed with paired Student's *t*-tests.

Human intestinal tissue specimens. Human tissue specimens were obtained from patients who underwent surgery for the treatment of Crohn's disease, UC, or colon cancer at Yokohama Municipal General Hospital or Tokyo Medical and Dental University Hospital. Written informed consent was obtained from each patient, and the study was approved by the ethics committee of Yokohama Municipal General Hospital and Tokyo Medical and Dental University.

Immunohistochemistry. Immunohistochemistry using intestinal tissues has been described elsewhere (12). The same antibodies used in immunoblot analysis were also used for the immunohistological staining of NICD1 and Hes1. The other antibodies used were anti-human Ki-67 (1:50, MIB-1, DAKO), anti-human PLA2G2A (1:200, sc-14468, Santa Cruz Biotechnology), anti-human MUC2 (1:100, Ccp58, Santa Cruz Biotechnology), and anti-mouse Ki-67 (1:50, TEC-3, DAKO). Microwave treatment (500 W, 10 min) in 10 mM citrate buffer was required for staining human tissues in Hes1, Ki-67, and NICD1 and for staining mice tissues in Ki-67. The tyramide signal amplification (Molecular Probes) was used for immunofluorescent detection of NICD1. Staining was visualized by an avidin-biotin-peroxidase complex (ABC) elite kit (Vector) using diaminobenzidine as a substrate or by secondary antibodies conjugated with Alexa-594 or Alexa-488 (Molecular Probes). The quantification of Hes1 (Fig. 1*B*), Alcian blue, Ki-67, or NICD1 (Fig. 8*B*) was conducted by the examination of nine randomly selected longitudinal sections of crypts selected from at least three different individuals. The data were statistically analyzed with paired Student's *t*-tests.

Microarray. Microarray analysis was performed using the Acegene human oligo chip 30K subset A (Hitachi software). Total RNA was collected before and after 24 h of NICD1 expression in LS174T cells and labeled using the Amino Aryll Message Amp aRNA kit (Ambion). The complete dataset of the analysis has been submitted to the NCBI Gene Expression Omnibus (GEO) and is accessible through GEO accession number GSE10136.

Table 1. *Primers used in the present study*

Gene	Primer Sequence	
	Forward	Reverse
Human Hes1	5′- ATGCCAGCTGATATAATGGAG -3′	5′- TCACCTCGTTCATGCACTCG -3′
Human Notch1	5′- CCGAACCAATACAACCCTCT -3′	5′- GCGATCTGGGACTGCTGCATGCT -3′
Human PLA2G2A	5′- ACCATGAAGACCCTCCTACTG -3′	5′- GAAGAGGGGACTCAGCAACG -3′
Mouse Hes1	5′- TCAACACGACACCGGACAAACC -3′	5′- GGTACTTCCCCAACACGCTCG -3′
Mouse MUC2	5′- TCCACCATGGGGCTGCCACT -3′	5′- GGCCCGAGAGTAGACCTTGG -3′
Mouse TNF-α	5′- CTACTGGCGCTGCCAAGGCTGT -3′	5′- GCCATGAGGTCCACCACCCTG -3′
Mouse IFN-γ	5′- ACACTGCATCTTGGCTTTGC -3′	5′- CGGATGAGCTCATTGAATGCT -3′
MouseIL-1α	5′- CCCGTCCTTAAAGCTGTCTG -3′	5′- AATTGGAATCCAGGGGAAAC -3′
Mouse IL-1β	5′- TTGACGGACCCCAAAAGAT -3′	5′- GAAGCTGGATGCTCTCATCTG -3′
Mouse IL-6	5′- GCTACCAAACTGGATATAATCAGGA -3′	5′- CCAGGTAGCTATGGTACTCCAGAA -3′
Mouse PLA2G2A	5′- AAGAAGCCCAAATGCTGAAA -3′	5′- TTTATCACCGGGAAACTTGG -3′
Mouse β-actin	5′- CCTAAGGCCAACCGTGAAAAG -3′	5′- TCTTCATGGTGCTAGGAGCCA -3′

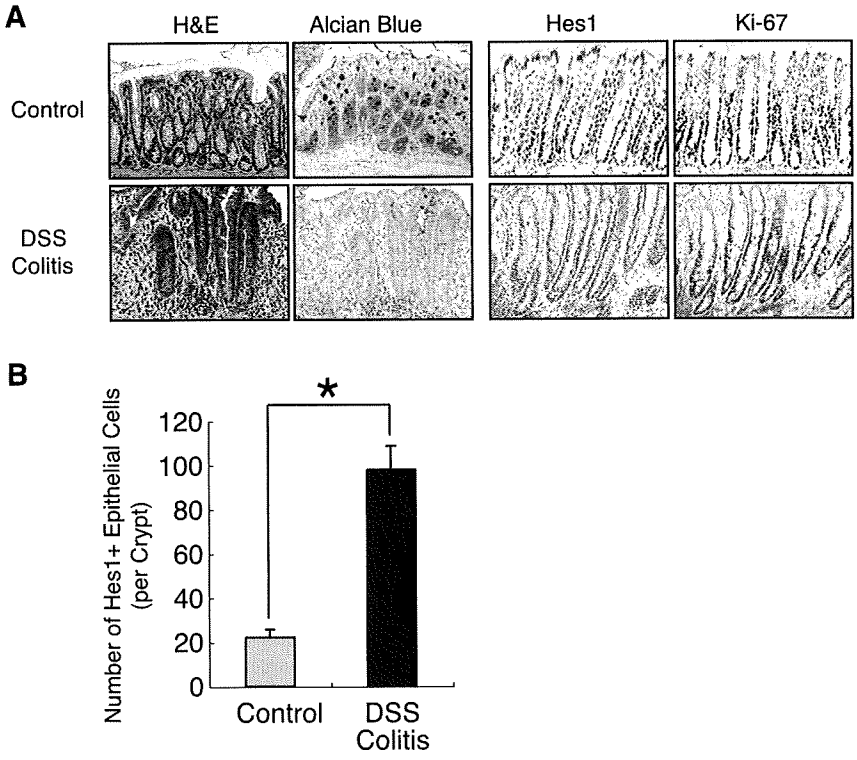

Fig. 1. Activation of Notch signaling is increased in crypts of dextran sodium sulfate (DSS)-induced colitis. *A*: histological analysis of DSS-induced colitis showing a decrease in mucin-producing intestinal epithelial cells (IECs) and an increase in Hes1- and Ki-67-expressing IECs within the crypts of the colitic mucosa. Blue staining with Alcian blue represents mucin production, whereas brown staining with diaminobenzidine (DAB) shows positive staining for Hes1 or Ki-67 (original magnification ×400). *B*: quantitative analysis of Hes1-positive IECs in crypts of normal or colitic mucosa. Data are shown as number of Hes1-positive cells per crypt on the basis of the analysis of immunohistochemical stainings. Error bars represent SD. $*P < 0.05$ on the Student's *t*-test. H & E, hematoxylin and eosin.

Plasmids. Hes1p-Luc, containing six tandem-repeats of the RBP-Jk binding site, was a kind gift from Dr. Kageyama (Kyoto, Japan). PLA2-Luc was generated by cloning a 2778-bp sequence 5′ of the human PLA2G2A gene (corresponding to −2,758 to + 20 of the promoter region) into a pGL3 basic vector (Promega). MUC2-Luc (40) was a kind gift from Dr. Yuasa (Tokyo, Japan). Tetracycline-dependent expression of NICD1 was achieved by cloning the gene encoding the intracellular portion of the mouse Notch1 (amino acid 1,704-2,531) into the pcDNA4/TO/myc-his vector (Invitrogen). All constructs were confirmed by DNA sequencing.

Immunostaining of cultured cells. Staining of cultured cells has been previously described (30). Detection of the MUC2 antibody was carried out either by the standard ABC method or by the Alexa 594-conjugated secondary antibody (Molecular Probes). The quantification of cells positive for MUC2 staining was performed by examining six randomly selected fields (three fields each in two individual counts) under ×400 magnification. The data were statistically analyzed with paired Student's *t*-tests.

ELISA. For PLA2G2A protein quantification, 1×10^6 cells were cultured in 2 ml of medium with or without DOX and analyzed with the human-PLA2 enzyme immunoassay kit (Cayman Chemicals). The incorporation of BrdU was examined by seeding cells at various cell densities in the 96-well plate, supplemented with DMSO or LY411,575. The BrdU was added 8 h before the end of culture, and the cells were subjected to analysis with the cell proliferation ELISA kit (Roche Diagnostics). The results are shown as the means of data collected by two rounds of assays, with each assay performed in triplicate. The data were statistically analyzed with paired Student's *t*-tests.

Reporter assays. The reporter assay was performed as previously described (18). Each assay was performed in triplicate, and the results were normalized using the *Renilla* luciferase activity. The results are shown as the means of normalized arbitrary units, and the data were statistically analyzed with paired Student's *t*-tests.

RESULTS

Hes1 is expressed in crypt epithelial cells of DSS-colitis. Since previous studies have evaluated the contribution of Notch signaling in the maintenance of mice intestinal epithelium (28, 33, 34), we sought to examine the role of Notch signaling in mice colitis. At first, we analyzed the expression of Hes1, a direct target gene of Notch, in mice with colitis induced by the oral administration of DSS (DSS-colitis, Fig. 1*A*). In the normal colon, crypts are predominantly composed of mature goblet cells that produce mucin. In such crypts, Hes1 is expressed in IECs residing at the lowest part of the crypt, which is also where Ki-67-positive IECs are found. In sharp contrast, the clear loss of mucin production was observed in the inflamed mucosa of DSS-colitis mice. The expressions of both Hes1 and Ki-67 were observed in a larger population of IECs, which were distributed from the bottom to the most upper regions of the crypt, suggesting that Notch signaling was activated in these IECs. The quantitative analysis of the immunostaining revealed significant increases in Hes1-positive IECs within the crypts of the DSS-colitis mice (Fig. 1*B*). These findings suggested that Notch signaling is activated in a greater number of IECs in DSS-colitis, which might be closely related with the greater number of proliferating IECs and the loss of mucin-producing IECs.

LY411,575 inhibits Notch activation and promotes goblet cell differentiation in mice intestine. To further examine the role of Notch signaling in colitis, we used LY411,575, a γ-secretase inhibitor (GSI) that is known to block Notch activation in vivo (14, 27, 36). Oral administration of LY411,575 for 5 consecutive days significantly reduced the expression of

Hes1 mRNA in mice intestine, suggesting that Notch activation was inhibited (Fig. 2*A*). In contrast, the expression of MUC2 mRNA was significantly increased by LY411,575, suggesting that the number of goblet cells increased. Consistent with this, histological analysis showed marked increases in mucus-producing IECs in the intestines of the LY411,575-treated mice (Fig. 2*C*). Consistent with reports from previous studies (27, 36), these results showed that LY411,575 could

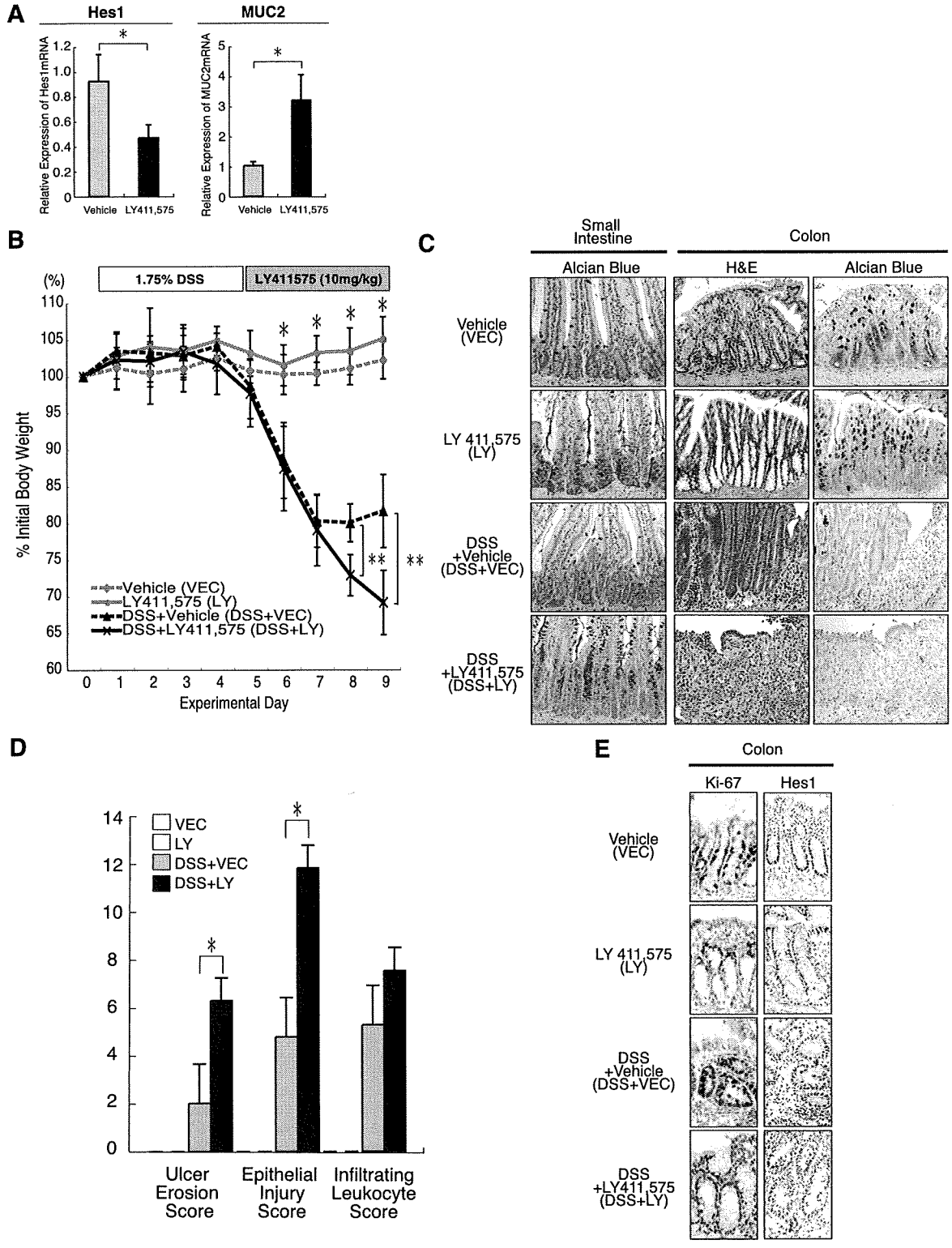

simultaneously inhibit Notch activation and promote differentiation to goblet cells in the mice intestine.

We also found marked atrophy of the thymus in LY411,575-treated mice (Supplemental Fig. S1*A*). Supplemental data for this article are available on the *American Journal of Physiology Gastrointestinal and Liver Physiology* website. Further analysis of the thymus revealed that the total number of thymocytes was significantly reduced (Supplemental Fig. S1*B*) and that the tissue architecture was disrupted (Supplemental Fig. S1*C*). Analysis of CD4/CD8 expression revealed a significant proportional reduction in double-positive cells (Supplemental Fig. S1*D*) and a reduction in the absolute number of cells (Supplemental Fig. S1*E*), suggesting that there was a significant loss of immature cells in the thymus with LY411,575 treatment. However, such an effect of LY411,575 was not present in the spleen (Supplemental Fig. S1, *A–E*). These findings clearly showed that the LY411,575 treatment had a systemic effect, affecting the thymus in addition to the intestine.

LY411,575 exacerbates DSS-colitis by impairing epithelial regeneration. Using the methods described, we designed an experiment to examine the effect of Notch inhibition during colitis (Fig. 2*B*). Mice were separated into four groups: vehicle alone (VEC), LY411,575 alone (LY), DSS with vehicle (DSS + VEC), and DSS with LY411,575 (DSS + LY). As of *day 5*, the total body weights showed significant reductions from *day 0* in DSS-treated mice (Fig. 2*B*) compared with the weights of those without DSS (the day when DSS treatment was started is designated as *day 0*). However, the DSS + LY mice showed even greater reductions in weight as of *day 8*; their reductions in body weight were significantly greater than the weight reductions in DSS + VEC mice (Fig. 2*B*). This severe loss of body weight observed in DSS + LY mice was also fatal because two mice in this group were dead at the time of euthanasia (fatality rate = 2/6, 33.3%). No deaths were observed in any other experimental group. These results suggested that LY411,575 significantly exacerbates the clinical course of DSS-colitis. A histological analysis of LY or DSS + LY mice showed a marked increase in goblet cells in the small intestine, confirming the effect of LY411,575 treatment (Fig. 2*C*). The increase in goblet cells was also observed in the colon of LY mice. A histological analysis of DSS + VEC mice showed a clear induction of colitis, as shown by the marked increase in inflammatory cells and the elongation of goblet cell depleted crypts. However, in sharp contrast, DSS + LY mice showed a severe loss of the epithelial layer in addition to an infiltration of inflammatory cells, which appeared to lack signs of epithelial regeneration (Fig. 2*C*). A histological scoring of the colonic tissues revealed increased ulcer formation and epithelial injury in DSS + LY mice compared with DSS + VEC mice, whereas no significant changes were observed in the degree of inflammation (Fig. 2*D*). Consistent with this, the mRNA expression of proinflammatory cytokines was increased in the colon of DSS-treated mice, but no clear differences were observed between DSS + VEC and DSS + LY mice (Supplemental Fig. S2).

For further analysis, we examined the expression of Hes1 and Ki-67 in the inflamed region of the colonic tissues. An increase in Hes1- or Ki-67-positive IECs was confirmed in DSS + VEC mice (Fig. 2*E*). However, both Hes1 and Ki-67 expression appeared to be markedly lost in the colonic crypts upon LY411,575 treatment (Fig. 2*E*). These results indicated that LY411,575 inhibits Notch activation and promotes goblet cell differentiation but also strongly inhibits proliferation of IECs, leading to a poor regenerative response and a severe exacerbation of DSS-colitis.

LY411,575 promotes goblet cell differentiation but inhibits proliferation of IECs in vitro. Previous in vivo results suggested that Notch activation might play critical roles in both the differentiation and proliferation of IECs. We further examined the in vitro effect of LY411,575 upon human colonic epithelial cell lines LS174T and HT29. As shown by the immunoblot analysis, the endogenous expression of both NICD1 and Hes1 was completely inhibited within LS174T cells by LY411,575 treatment (Fig. 3*A*). Consistent with this, RT-PCR analysis showed a marked decrease in Hes1 mRNA expression with LY411,575, which was maintained for up to 72 h (Fig. 3*B*). These data confirmed that LY411,575 could directly inhibit the activation of Notch within IECs.

Under this condition, we examined whether LY411,575 could promote goblet cell differentiation in vitro. Quantitative RT-PCR analysis showed a significant increase in MUC2 mRNA expression with LY411,575 treatment in both LS174T and HT29 cells (Fig. 3*C*). Consistent with this, a marked induction of MUC2 protein expression was observed in both of the cell lines that were treated with LY411,575 (Fig. 3*D*, red signal), resulting in a significant increase in the MUC2-positive cell population (Fig. 3*E*). The Alcian blue staining also showed a marked increase in mucin-producing cells in both cell lines with LY411,575 (Fig. 3*F*, black arrow). However, LY411,575 appeared to inhibit the proliferation of both cell lines since the incorporation of BrdU was significantly downregulated by LY411,575 (Fig. 3*G*). These results collectively showed that LY411,575 could directly inhibit Notch activation in IECs, which might subsequently promote goblet cell differentiation but also inhibit cell proliferation.

Activation of Notch1 suppresses goblet cell phenotype, but upregulates PLA2G2A secretion in human IECs. To further analyze the function of Notch activation in IECs, we gen-

Fig. 2. Inhibition of Notch activation by LY411,575 exacerbates DSS-colitis by impairing epithelial regeneration. *A*: LY411,575 suppresses Hes1 expression but also promotes MUC2 expression in mice intestine. After oral administration of LY411,575 or vehicle alone for 5 consecutive days, the small intestinal tissues of mice were subjected to quantitative RT-PCR analysis. Results from 3 mice in each group. Error bars represent SD. $*P < 0.05$ on the Student's *t*-test. *B*: LY411,575 significantly exacerbated wasting disease caused by DSS. As described in MATERIALS AND METHODS, mice were separated into 4 groups, and the body weight of each mouse was monitored throughout the experimental period. Error bars represent SD. $*P < 0.05$ for the difference between mice that were DSS treated (DSS + VEC and DSS + LY) or not treated (VEC and LY). $**P < 0.05$ for the difference between DSS + VEC and DSS + LY mice on the Student's *t*-test. *C*: LY411,575 exacerbated epithelial injury of DSS-colitis. Intestinal tissues of mice shown in *B* were subjected to histological analysis. Blue staining with Alcian blue represents mucin production (original magnification ×400). *D*: LY411,575 had no significant effect on inflammation of DSS-colitis. Histological scoring of colonic tissues obtained from each mice group is shown. Error bars represent SD. $*P < 0.05$ on the Student's *t*-test. *E*: LY411,575 inhibited proliferation of IECs via downregulation of Notch activity. Colonic tissues of mice were subjected to immunohistochemical staining for Hes1 and Ki-67. A less inflamed region was chosen for analysis of DSS + LY mice because the most inflamed region showed complete loss of the epithelial layer. Note that IECs expressing Hes1 or Ki-67 were confined within a narrow region of the colonic crypt in mice treated with LY411,575 (LY and DSS + LY).

erated a subline of LS174T cells (Tet-On NICD1 cells), in which forced expression of NICD1 could be induced in a tetracycline- or DOX-dependent manner. Immunoblot analysis of Tet-On NICD1 cells showed a clear induction of NICD1 and a subsequent increase in Hes1, with DOX addition (Fig. 4*A*). Consistent with this, the reporter activity of Hes1p-Luc was significantly upregulated with the induction of NICD1 in Tet-On NICD1 cells, indicating that there was an upregulation of the transcriptional activity of the Hes1 gene (Fig. 4*B*). These results confirmed that Tet-On NICD1 cells could express the functional NICD1 protein with DOX addition.

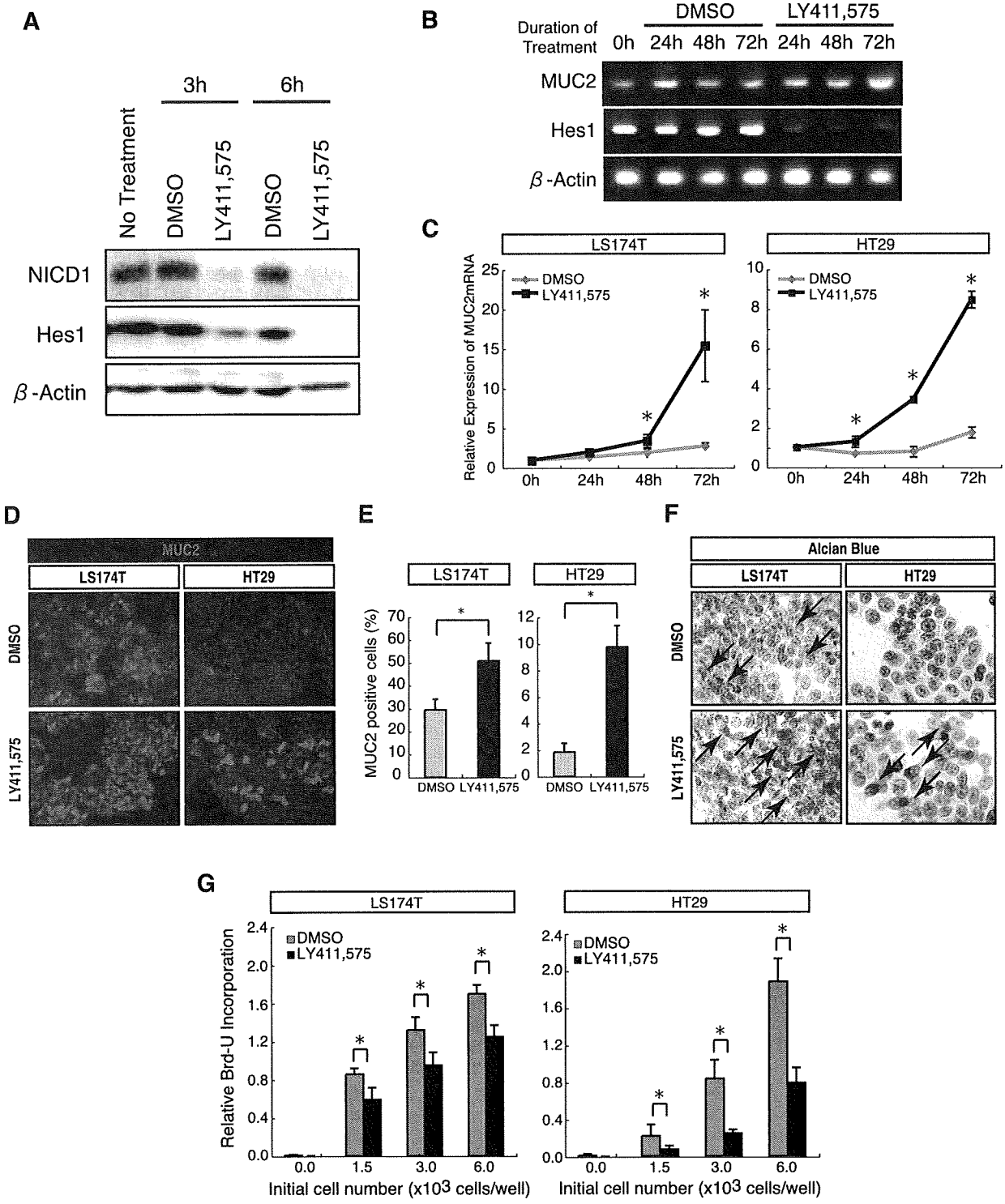

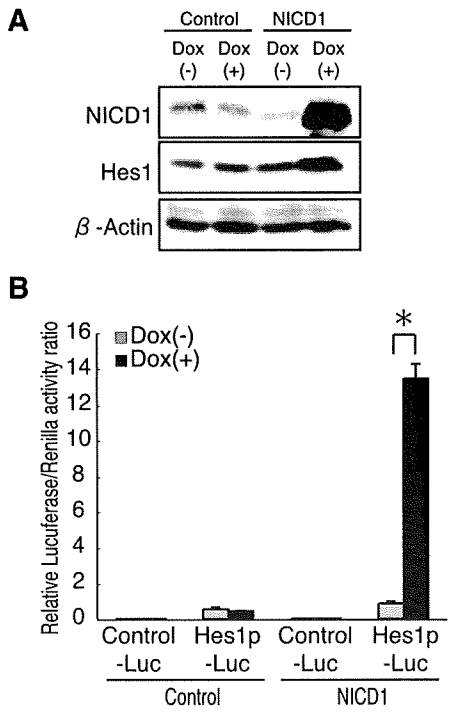

Fig. 4. Activation of Notch1 upregulates Hes1 expression in human IECs. *A*: establishment of a subline of LS174T cells expressing NICD1 under control of a tetracycline-dependent promoter (Tet-On NICD1 cells, designated as NICD1). Immunoblot analysis of Tet-On NICD1 cells showed a clear upregulation of both NICD1 and Hes1 expression with doxycycline (DOX) addition, whereas parental cells (designated as Control) remain unchanged. A low-sensitivity substrate (ECL) was used for visualization. *B*: transcriptional activity of Hes1 was upregulated with the expression of NICD1. Transcriptional activities of Hes1 gene in Tet-On NICD1 cells or control cells were analyzed by luciferase reporter assays using Hes1p-Luc. A reporter plasmid containing only the core-promoter of chicken β-actin gene served as a control (Control-Luc). Luciferase activities were measured after 12 h of culture with or without DOX. Error bars represent SD. $*P < 0.05$ on the Student's *t*-test.

Using this cell line, we found that the upregulation of NICD1 expression in LS174T cells significantly downregulated MUC2 mRNA expression (Fig. 5*A*). Further analysis with a microarray identified a group of genes that were up- or downregulated with NICD1 expression (Supplemental Tables 1 and 2). Among these genes, we focused on PLA2G2A, a gene expressed by Paneth cells, as it showed the most significant induction with NICD1 expression. Quantitative RT-PCR confirmed an upregulation of PLA2G2A mRNA expression with the NICD1 expression (Fig. 5*A*). Consistent with this, although the MUC2 protein expression was markedly suppressed (Fig. 5*B*), with resulting significant decreases in MUC2-positive cells (Fig. 5*C*) and mucin-producing cells (Fig. 5*D*), the PLA2G2A secretion was upregulated with NICD1 expression (Fig. 5*E*). These changes appeared to be regulated at the transcriptional level since the reporter activities of MUC2-Luc and PLA2-Luc showed a significant decrease and increase, respectively, with NICD1 expression (Fig. 5*F*). These results showed that, although the activation of Notch1 within LS174T cells suppressed goblet cell phenotype, it also upregulated the secretion of PLA2G2A, suggesting that the activation of Notch1 might surprisingly promote the acquisition of the specific functions of Paneth cells.

Notch1 is activated in crypt epithelial cells of the human intestine. Since we found that Notch signaling might regulate cell proliferation, goblet cell differentiation, and Paneth cell-specific function within IECs, we sought to clarify its relevance in human intestinal diseases. We first examined whether components of the Notch signaling pathway are expressed in the human intestine. An RT-PCR analysis of human intestinal tissues or epithelial cell lines successfully detected mRNAs of both Notch1 and Hes1 (Fig. 6*A*). The immunohistochemistry for NICD1 and Hes1 revealed that these proteins are expressed in the nuclei of crypt IECs (Fig. 6*B*). Similar to our observations in mice, the distribution of NICD1-positive or Hes1-positive IECs corresponded to that of Ki-67-positive IECs (Fig. 6*B*). Also, a magnified view of the staining showed a positive staining of NICD1 in columnar-shaped IECs and Paneth cells (Fig. 6*B*, black arrow) but not in goblet-shaped IECs (Fig. 6*B*, red arrowhead). Double staining of MUC2 and NICD1 confirmed the lack of NICD1 expression in goblet cells (Fig. 7*A*), whereas double staining of PLA2G2A and NICD1 confirmed expression of NICD1 in Paneth cells (Fig. 7B). These results strongly suggested that the NICD1 might function in vivo in the human intestine in a similar manner as was revealed in the in vitro study.

Increased activation of Notch1 is observed in the mucosa of UC. UC is one of the major forms of inflammatory bowel diseases, characterized by the persistent inflammation and ulcer formation in the colon. In the active region of UC, a loss of goblet cells, an ectopic expression of Paneth cell genes, and an increase in IEC proliferation are all known to be common pathological findings (7, 8, 13, 23). Thus our results strongly suggested that all of these pathological findings in UC might be mediated by the activation of Notch1 in IECs. We performed

Fig. 3. Inhibition of Notch activation promotes differentiation of goblet cells but suppresses proliferation of human IECs. *A*: LY411,575 downregulated expression of Notch1 intracellular domain (NICD1) and Hes1 in LS174T cells. Immunoblot analysis of LS174T cells treated with LY411,575 showing downregulation of endogenous NICD1 and Hes1 expression within 6 h from treatment. Cells treated with DMSO alone served as control. A high-sensitivity substrate (ECL Advance) was used for visualization. *B*: LY411,575 upregulated expression of MUC2 in LS174T cells. LS174T cells were subjected to semiquantitative RT-PCR analysis after treatment with either LY411,575 or DMSO. Note that expression of Hes1 was markedly decreased, whereas expression of MUC2 was increased after 72 h of treatment with LY411,575. *C*: LY411,575 significantly increased expression of MUC2 mRNA in both LS174T and HT29 cells. Cells were subjected to quantitative RT-PCR analysis after 0, 24, 48, and 72 h of treatment with either LY411,575 or DMSO. Error bars represent SD. $*P < 0.05$ for the difference between DMSO and LY411,575 treatment at the same time points on the Student's *t*-test. *D*: LY411,575 induced expression of MUC2 protein (red) in LS174T and HT29 cells. Cells were subjected to immunofluorescent staining of MUC2 after 72 h of treatment with either LY411,575 or DMSO (original magnification ×200). *E*: LY411,575 significantly increased the MUC2-positive cell populations among LS174T and HT29 cells. Quantitative analysis of *D* is shown by percent of MUC2-positive cells within total nucleated cells. Error bars represent SD. $*P < 0.05$, on the Student's *t*-test. *F*: LY411,575 induced mucin production in LS174T and HT29 cells. Cells were subjected to Alcian blue staining (black arrow) after 72 h of treatment with either LY411,575 or DMSO (original magnification ×400). *G*: LY411,575 significantly downregulated proliferation of LS174T and HT29 cells. A significant decrease in BrdU incorporation was observed with LY411,575 treatment in LS174T and HT29 cells. Incorporation of BrdU was measured by ELISA. Results are shown as arbitrary units of relative BrdU incorporation. Error bars represent SD. $*P < 0.05$ on the Student's *t*-test.

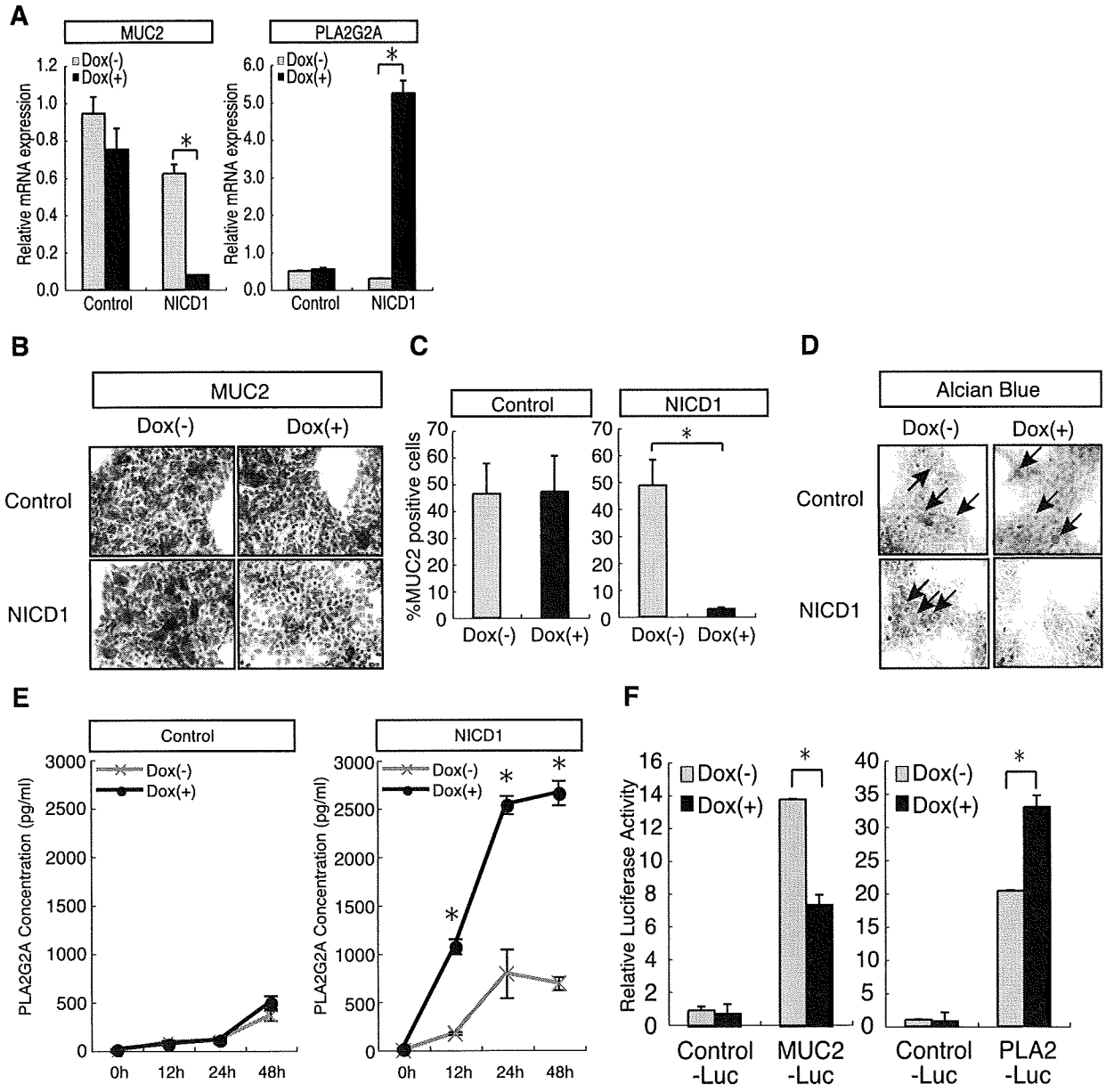

Fig. 5. Activation of Notch1 suppresses goblet cell differentiation but promotes expression of PLA2G2A of human IECs. *A*: expression of NICD1 in LS174T cells downregulated the expression of MUC2 but upregulated the expression of PLA2G2A. Quantitative RT-PCR analysis of MUC2 and PLA2G2A expression in Tet-On NICD1 cells and control cells is shown. Cells were subjected to analysis after 48 h of culture with or without DOX. Error bars represent SD. $*P < 0.05$ on the Student's *t*-test. *B*: expression of NICD1 in LS174T cells downregulated MUC2 protein expression. Tet-On NICD1 cells or control cells were subjected to immunostaining of MUC2 after 48 h of culture with or without DOX. Brown staining with DAB showed positive staining for MUC2 (original magnification ×200). *C*: expression of NICD1 in LS174T cells significantly reduced the number of cells expressing MUC2. Quantitative analysis of immunostaining shown in *B* is shown. Number of cells positively stained for MUC2 was counted and shown as percent of total nucleated cells. Error bars represent SD. $*P < 0.05$ on the Student's *t*-test. *D*: expression of NICD1 suppressed mucin production by LS174T cells. Tet-On NICD1 cells or control cells were treated as described in *B* and subjected to Alcian blue staining. The blue staining represents mucin-producing cells. (black arrow, original magnification ×800). *E*: expression of NICD1 upregulated PLA2G2A secretion of LS174T cells. Tet-On NICD1 cells or control cells were cultured with or without DOX, and culture supernatants collected at various time points were subjected to quantification of PLA2G2A using ELISA. Error bars represent SD. $*P < 0.05$ compared between DOX (+) and DOX (-) on the Student's *t*-test. *F*: expression of NICD1 in LS174T cells downregulated transcriptional activity of MUC2 gene but upregulated transcriptional activity of PLA2G2A gene. Transcriptional activity of MUC2 gene and PLA2G2A gene were measured by luciferase reporter assays using MUC2-Luc and PLA2-Luc as a reporter plasmid, respectively. pGL3-basic served as a control (Control-Luc). Luciferase activities in Tet-On NICD1 cells were analyzed after 12 h of culture with or without DOX. Error bars represent SD. $*P < 0.05$ on the Student's *t*-test.

histological analysis and found that in the crypts of UC, mucin production is markedly decreased (Fig. 8*A*, *top*, blue), whereas the number of Ki-67-expressing cells are markedly increased, distributing from the bottom to the uppermost part of the crypt (Fig. 8*A*, *bottom*, brown). In such crypts, NICD1-expressing cells showed the same distribution as Ki-67-expressing cells (Fig. 8*A*, *middle*, brown), suggesting that Notch1 is activated in an expanded proliferating cell population within the crypts of

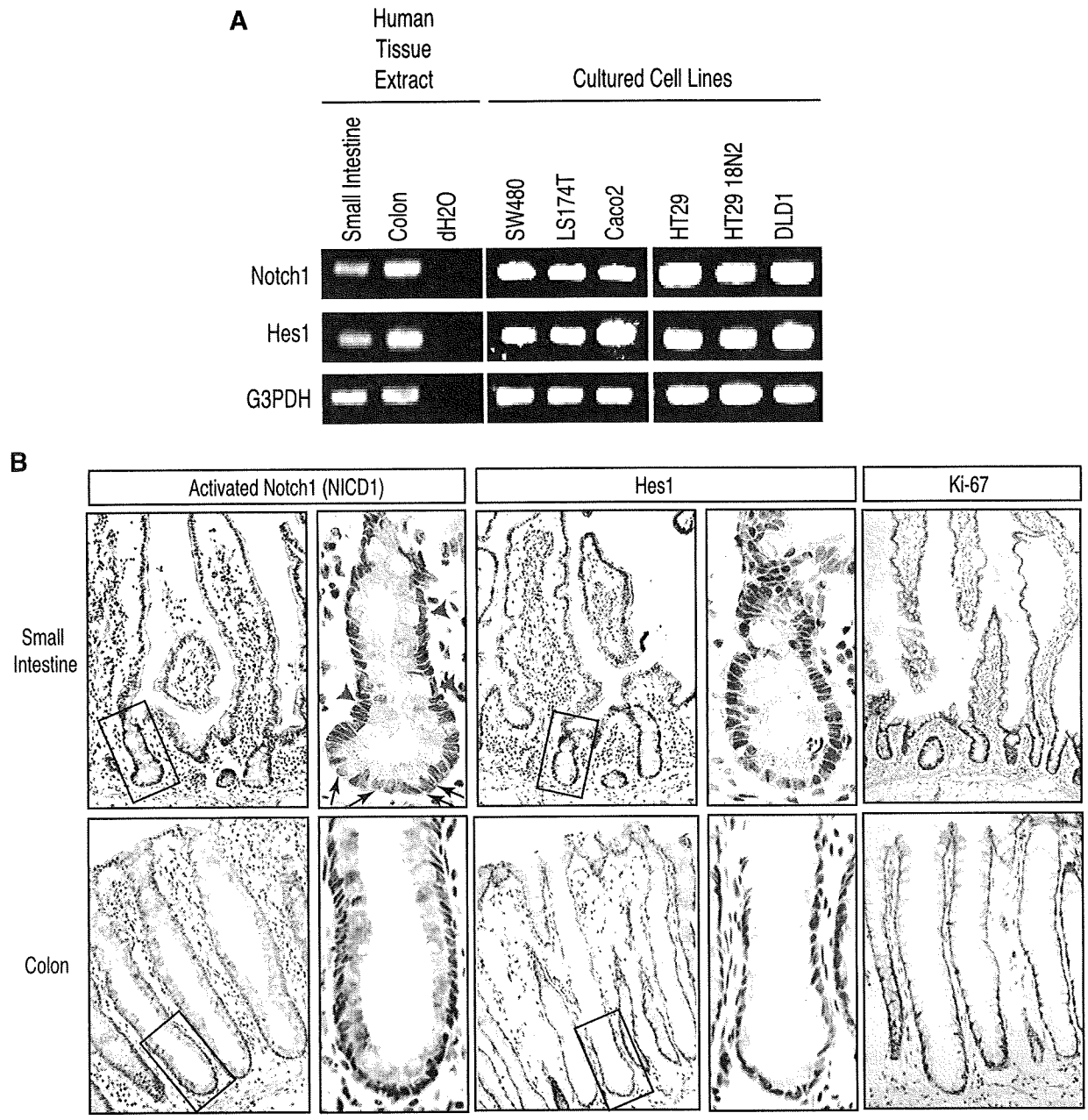

Fig. 6. Notch signaling is activated in crypt epithelial cells of the human intestine. *A*: RT-PCR analysis of human intestinal tissues and human intestinal epithelial cell lines. Expression of both Notch1 and Hes1 are clearly detected in all the examined tissues and cell lines. *B*: immunostaining of human intestinal tissues showing expression of NICD1, Hes1, and Ki-67. Brown staining with DAB showed positive results for NICD1, Hes1, and Ki-67 (original magnification ×200). Magnified view of the squared area is shown in the right side of the original picture (original magnification ×1000). Black arrows show Paneth cells clearly containing granules in the cytoplasm showing positive staining for NICD1, whereas red arrowheads show goblet-shaped cells lacking NICD1 staining.

UC. A quantitative analysis revealed that the number of IECs expressing NICD1 or Ki-67 per crypt is significantly increased, whereas the number of IECs producing mucin is significantly decreased in the crypts of UC (Fig. 8*B*).

We also looked for IECs expressing PLA2G2A within the colonic crypts. There was no expression of PLA2G2A in the crypts of the normal colon (Fig. 9*A*). However, an ectopic expression of PLA2G2A was clearly found in the crypts of the colon epithelia with UC (Fig. 9*B*). Our histological analysis revealed that Notch1 is clearly activated in such IECs ectopically expressing PLA2G2A (Fig. 9, *C* and *D*). Such activation of Notch1 in PLA2G2A-expressing cells could also be found in less inflamed regions of UC where there were fewer PLA2G2A-expressing IECs (Fig. 9, *E* and *F*).

From these results, we confirmed that Notch1 is activated in a greater number of crypt IECs in UC, presumably mediating goblet cell depletion, cell proliferation, and ectopic expression of PLA2G2A. We suggest that such Notch1-mediated changes

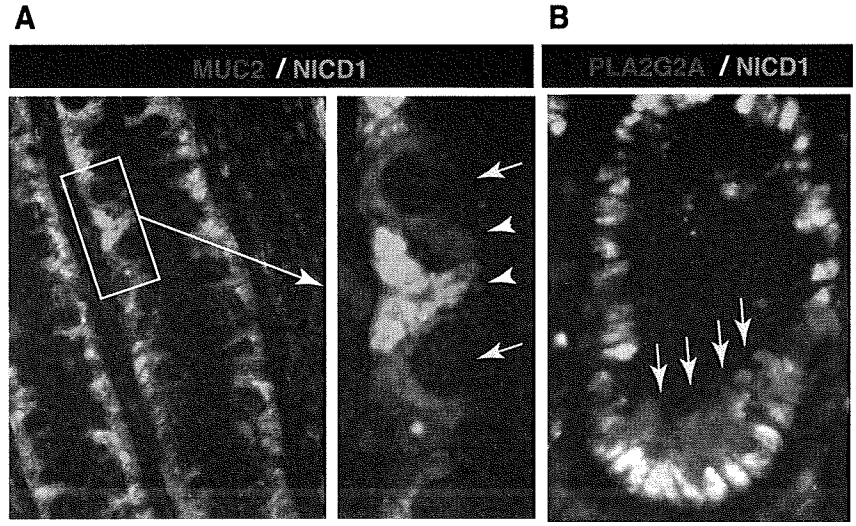

Fig. 7. Human Notch1 is not activated in IECs expressing MUC2 but is activated in IECs expressing PLA2G2A. *A*: human Notch1 was not activated in IECs expressing MUC2 in vivo. Double staining for MUC2 (red) and NICD1 (green) using human colonic tissue is shown. NICD1 and MUC2 were expressed in distinct populations of epithelial cells (*left*, ×400). A magnified view (*right*, ×1600) clearly shows cytoplasmic staining of MUC2 in goblet-shaped cells (yellow arrow), whereas nuclear staining of NICD1 in columnar-shaped cells (white arrowhead). *B*: human Notch1 is activated in IECs expressing PLA2G2A in vivo. Double staining for PLA2G2A (red) and NICD1 (green) using a human small intestinal tissue is shown. NICD1 and PLA2G2A were coexpressed in IECs residing at the lowest part of the crypt, suggesting activation of Notch1 in Paneth cells (yellow arrow, original magnification ×1000).

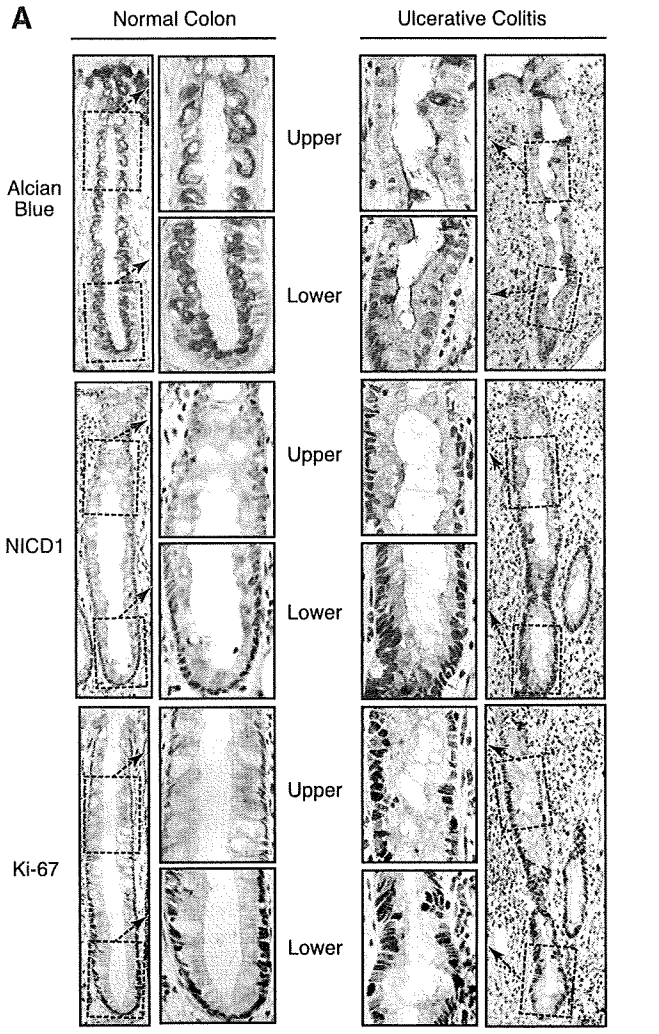

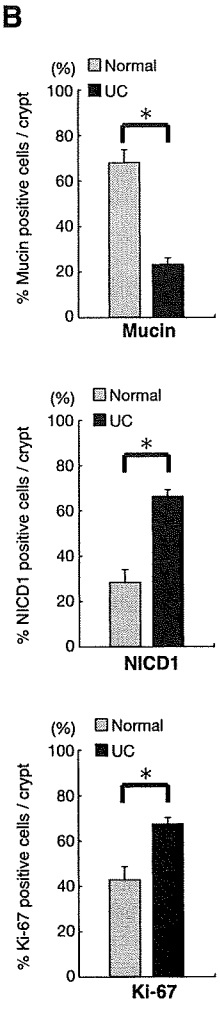

Fig. 8. Increased activation of Notch1 is observed in the crypts of patients with ulcerative colitis (UC). *A*: decreased expression of mucin and increased expression of both NICD1 and Ki-67 were observed in crypts of patients with UC. Mucin expression was examined by Alcian blue staining, whereas expression of NICD1 or Ki-67 was examined by immunohistochemistry with the use of human colonic tissues. Inner column shows magnified view of the upper (Upper) and lower (Lower) crypt areas identified by dashed line in the outer column. A marked decrease in Alcian blue-positive IECs is observed in a crypt of a patient with UC (*top*). In contrast, a marked increase in IECs expressing NICD1 (brown, *middle*) or Ki-67 (brown, *bottom*) was observed in patients with UC. Distribution of IECs expressing NICD1 or Ki-67 was restricted to the lower part of the crypt in normal colon, but it extended to the most upper region of the crypt in UC (original magnification, outer column ×400, inner column ×1600). *B*: significant decrease in IECs expressing mucin and significant increase in IECs expressing NICD1 or Ki-67 were observed in crypts of patients with UC. Quantitative analysis of the histological staining for mucin, NICD1, and Ki-67 is shown. Number of IECs positive for Alcian blue staining or immunohistochemical staining for NICD1 and Ki-67, respectively, were counted per crypt and normalized by total number of IECs. Results are shown as percent positive IECs per crypt. Error bars represent SD. $*P < 0.05$ on the Student's *t*-test.

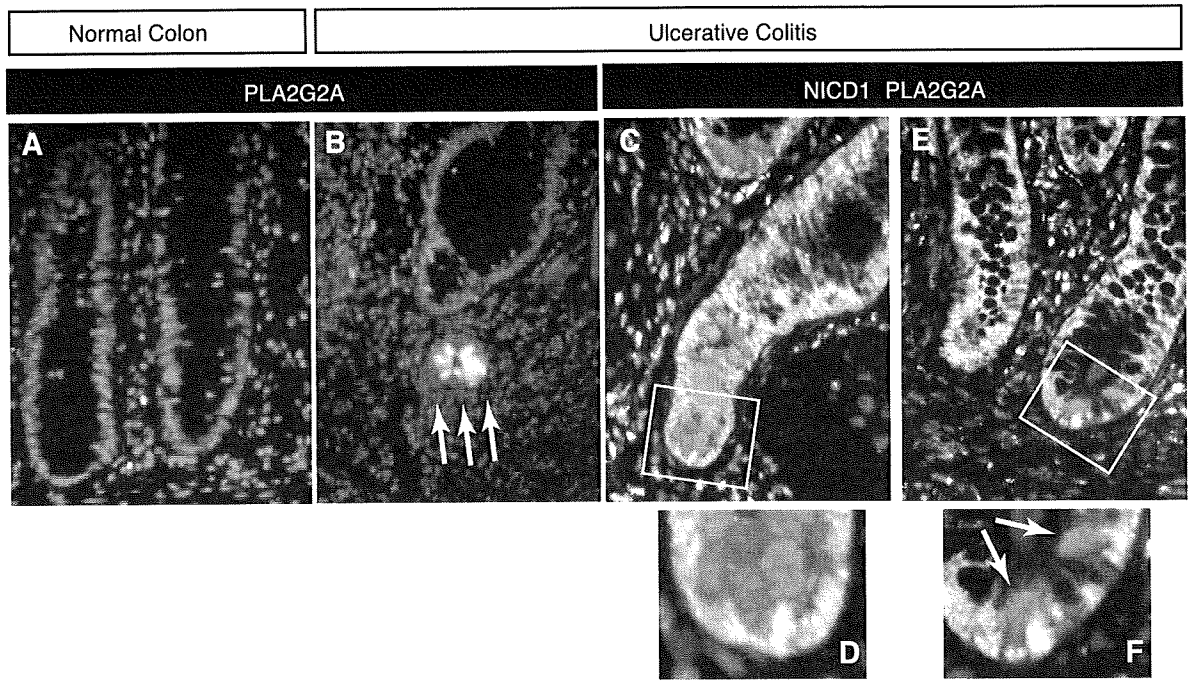

Fig. 9. Notch1 is activated in IECs ectopically expressing PLA2G2A. Fluorescent immunostaining for PLA2G2A (red) was completely negative in the crypts of normal colon (*A*, original magnification ×400), whereas some of the IECs in the crypts of a patient with UC were clearly positive for PLA2G2A (*B*, yellow arrow, original magnification ×400). Some cells in the lamina propria were also positive for PLA2G2A. Double immunostaining for NICD1 (green) and PLA2G2A (red) showed coexpression of NICD1 and PLA2G2A by colonic IECs of a patient with UC (*C–F*). In the inflamed region (*C*, *D*), NICD1 was expressed in most parts of the crypt IECs, and some proportion of those IECs coexpressed PLA2G2A (*C*, original magnification ×400). A magnified view (*D*, original magnification ×1000) of the indicated region (white square in *C*) clearly showed a nuclear distribution of NICD1 and a cytoplasmic distribution of PLA2G2A. In a less inflamed region, few IECs appeared to be positive for both NICD1 and PLA2G2A (*E*, original magnification ×400). Magnified view of the indicated region (white square in *E*) confirms coexpression of NICD1 and PLA2G2A in the nucleus and cytoplasm of an IEC, respectively (*F*, yellow arrow, original magnification ×1000).

observed in the mucosa of UC are not detrimental changes contributing to the persistence of the disease, but rather they are positive responses that help to regenerate the damaged epithelia, thereby aggressively contributing to the termination and recovery from the disease.

DISCUSSION

To date, several studies using knockout mice have revealed various functions of Notch signaling in IECs; one critical function is that of regulating the cell fates of IECs (31). The recent model accepted in such studies implicates Notch activation as a positive regulator of absorptive cell differentiation but a negative regulator of the differentiation of secretory lineage cells, including goblet cells. However, studies have suggested that Notch activation not only acts to determine the cell fates of progenitor IECs, but it may also regulate the number of proliferating populations within the crypt (6, 28, 33). Our results are consistent with the previous observations, and they further highlight the critical role of Notch activation in a situation when the rapid expansion of IECs is required (e.g., during the regeneration process in UC). Since the in vivo phenotype of Notch inhibition showed not only the loss of absorptive lineage cells but also the loss of the entire epithelial layer, this suggested that the activation of Notch may contribute to the expansion of both absorptive and secretory precursor cells and even stem cells. This is consistent with the observation by Vooijs et al. (34) that IECs that matured into absorptive cells must have also experienced Notch activation during development from the stem cell. Thus our results demonstrated the importance of Notch activation in the expansion of multilineage precursor IECs, whose function becomes critically required when tissue damage is present. In contrast, although Notch activation was predominant in the proliferating IECs of the colitic mucosa, its role in postmitotic IECs might be of less importance (42).

A recent study has shown that the chronic inhibition of Notch activation using LY411,575 (for up to 15 consecutive days) could impair the development of lymphoid cells (14, 36). Thus it may be possible that such an effect of LY411,575 might have altered the local immune function of the DSS-treated mice and thereby exacerbated their colitis. Indeed, LY411,575 proved to have a systemic effect, especially on the development of thymocytes (Supplemental Fig. S1). However, no effect was observed on splenocytes (Supplemental Fig. S1). Also, no effect was observed on local production of proinflammatory cytokines (Supplemental Fig. S2). Thus, although it is possible that LY411,575 might have some effect on the inflammatory response, its involvement on the exacerbation of the present colitis model may be minimal.

Also, GSI has been reported to promote the differentiation and inhibit proliferation of mice intestinal adenoma through the inhibition of Notch activation (33). Therefore, GSIs have been reported to have an antitumor effect (32). However, our results showed that the effects of GSIs may not be specific for tumor